

# One Deep Music Representation to Rule Them All?

A comparative analysis of different representation learning strategies

Jaehun Kim · Julián Urbano ·  
Cynthia C. S. Liem · Alan Hanjalic

Received: date / Accepted: date

**Abstract** Inspired by the success of deploying deep learning in the fields of Computer Vision and Natural Language Processing, this learning paradigm has also found its way into the field of Music Information Retrieval. In order to benefit from deep learning in an effective, but also efficient manner, deep transfer learning has become a common approach. In this approach, it is possible to reuse the output of a pre-trained neural network as the basis for a new, yet unseen learning task. The underlying hypothesis is that if the initial and new learning tasks show commonalities and are applied to the same type of data (e.g. music audio), the generated deep representation of the data is also informative for the new task. Since, however, most of the networks used to generate deep representations are trained using a single initial learning task, the validity of the above hypothesis is questionable for an arbitrary new learning task. In this paper we present the results of our investigation of what the best ways are to generate deep representations for the data and learning tasks in the music domain. We conducted this investigation via an extensive empirical study that involves multiple learning tasks, as well as multiple deep learning architectures with varying levels of information sharing between tasks, in order to learn music representations. We then validate these representations considering multiple unseen learning tasks for evaluation. The results of our experiments yield several insights on how to approach the design of methods for learning widely deployable deep data representations in the music domain.

**Keywords** Representation Learning · Music Information Retrieval · Multi Task Learning

---

This work has been submitted to “Neural Computing and Applications: Special Issue on Deep Learning for Music and Audio” and currently is under review.

---

J. Kim, J. Urbano, C. C. S. Liem & A. Hanjalic  
Multimedia Computing Group  
Department of Intelligent Systems  
Faculty of Electrical Engineering, Mathematics and Computer Science  
Delft University of Technology  
Tel.: +31-15-27-87241  
E-mail: J.H.Kim@tudelft.nl

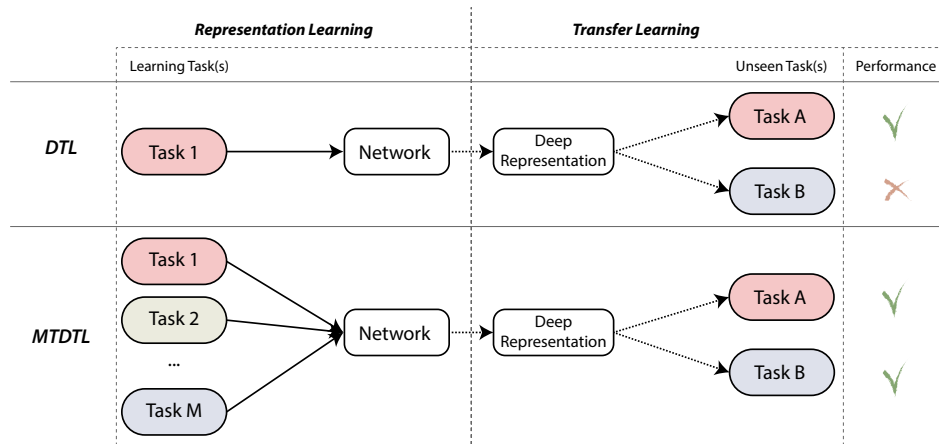


Fig. 1: Simplified illustration of the conceptual difference between traditional deep transfer learning (DTL) based on a single learning task (above) and multi-task based deep transfer learning (MTDTL) (below). The same color used for a learning and an unseen task indicates that the tasks have commonalities, which implies that the learned representation is likely to be informative for the unseen task. At the same time, this representation may not be that informative to another unseen task, leading to a low transfer learning performance. The hypothesis behind MTDTL is that relying on more learning tasks increases robustness of the learned representation and its usability for a broader set of unseen tasks.

## 1 Introduction

In the Music Information Retrieval (MIR) field, many research problems of interest involve the automatic description of properties of musical signals, employing concepts that are understood by humans. In order to move from raw audio content to humanly understood qualifiers (e.g. genre labels or descriptive tags), historically, the raw audio would first be transformed into a *representation* based on *hand-crafted features*. These features were engineered by humans to reflect dedicated semantic signal properties, after which they would serve as input to various statistical or machine learning approaches [1].

Following the successes in the fields of Computer Vision (CV) and Natural Language Processing (NLP), deep learning approaches have recently also gained increasing interest in the MIR field, in which case *deep representations* of music audio data are directly learned from the data, rather than being hand-crafted. Many works employing such approaches reported considerable performance improvements in various music analysis, indexing and classification tasks [2, 3, 4, 5, 6, 7].

In many deep learning applications, rather than training a complete network from scratch, pre-trained networks are commonly used to generate deep representations, which can be either directly adopted or further adapted for the current task at hand. In CV and NLP, (parts of) certain pre-trained networks [8, 9, 10, 11] have now been adopted and adapted in a very large number of works. These ‘standard’ deep representations have typically been obtained by training a network for a single learning task, such as visual object recognition, employing large amounts of training data. The hypothesis on why these representations are effective in a broader spectrum of tasks than they originally were trained for, is that *deep transfer learning (DTL)* is happening: information

initially picked up by the network is beneficial also for new (future, unseen) learning tasks performed on the same type of raw input data (i.e. images in this case). Clearly, the validity of this hypothesis is linked to the extent to which the new task can rely on similar data characteristics as the task on which the pre-trained network was originally trained. A number of works deployed DTL for various learning tasks in the music domain [12, 13], but based on a single selected learning task, which was not verified on optimal effectiveness for transfer learning against other options. An exception is [14], in which two different learning tasks were considered, although it was not justified why these particular two tasks were chosen.

In order to increase robustness to a larger scope of new learning tasks, the concept of Multi-Task Learning (MTL) has been applied in training deep networks for representation learning, both in the music domain [15] and in general [16, 17, 18, 19, 20, 21, 22, 23, 24]. In MTL, the network learns several tasks in parallel, so it may pick up commonalities among them. As a consequence, the expectation is that a deep representation learned with MTL will yield robust performance across different unseen tasks, by transferring shared knowledge [16]. A simple illustration of the conceptual difference between traditional DTL and deep transfer learning based on MTL (further referred to as *multi-task based deep transfer learning (MTDTL)*) is shown in Fig. 1.

The mission of this paper is to investigate what learning strategies will yield the most effective deep representations for typical data and learning tasks in the music domain. Here, we understand an ‘effective’ representation to be a representation that is suitable for a wide range of new learning tasks. We pursue this mission by investigating the effectiveness of MTDTL and traditional DTL, as well as concatenations of multiple deep representations, obtained by networks that were independently trained on separate single learning tasks. We consider these representations for multiple choices of learning tasks, and considering multiple evaluation tasks.

Our work will address the following research questions:

- **RQ1:** Given a set of common learning tasks that can be used to train a network, what is the influence of the number and type of the tasks on the effectiveness of the learned deep representation?
- **RQ2:** How do various degrees of information sharing in the deep architecture affect the ultimate success of a learned deep representation?
- **RQ3:** What is the best way to assess the effectiveness of a deep representation?

By answering the **RQ1** we arrive at a recommendation on *how to choose learning tasks*, both regarding their nature and their number, to generate an effective deep representation in the music domain. The answer to **RQ2** provides insight in *how to choose the optimal learning strategy* in terms of architecture setup. For example, in MTL, multiple tasks are considered under a joint learning scheme, that partially shares inferences obtained from different learning tasks in the learning pipeline. In MTL applications using deep neural networks, this means that certain layers will be shared between all tasks, while at other stages, the architecture will ‘branch’ out into task-specific layers [18, 19, 20, 21, 25, 26, 27]. However, investigation is still needed on where in the layered architecture branching should ideally happen—if a branching strategy would turn out strategic in the first place.

Finally, by answering **RQ3**, we help answer the question on *how to design and validate methods for deep representation learning*. For **RQ1**, we investigate different combinations of learning tasks. For **RQ2**, we study different architectural strategies. However, we wish to ultimately investigate effectiveness of the representation with respect to new, unseen learning tasks (which in the remainder of this paper will be denoted by *evaluation tasks*). While this may cause combinatorial explosion

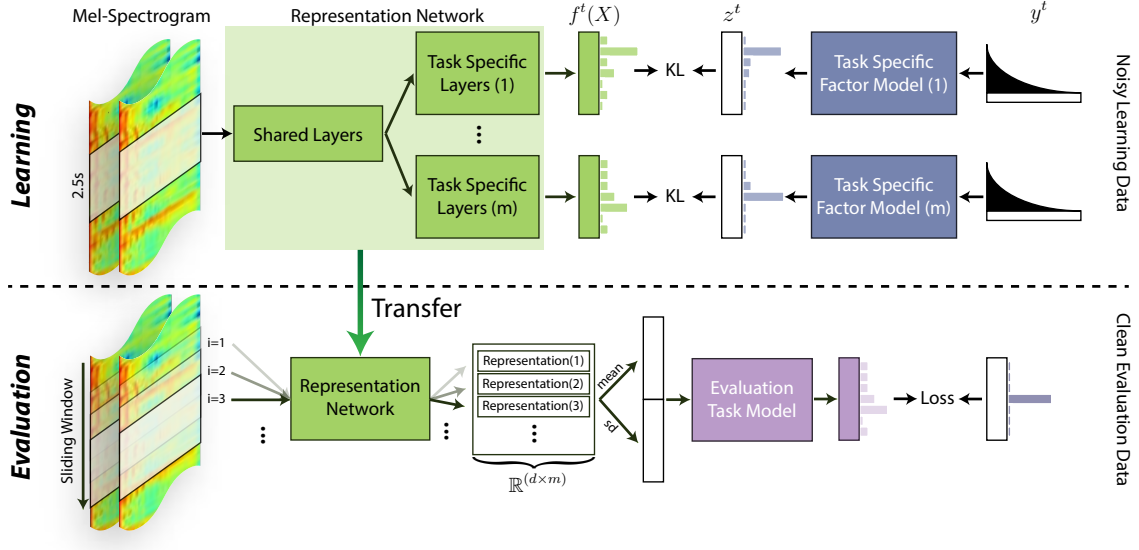


Fig. 2: Overall system framework.

with respect to possible experimental configurations, we will make strategic choices in the design and evaluation procedure of the various representation learning strategies.

The scientific contribution of this work can be summarized as follows:

- We provide insight into the effectiveness of a various deep representation learning strategies, and of the conditions under which this effectiveness is maximized.
- We offer in-depth insight into ways to evaluate desired properties of a deep-representation-learning procedure.
- We propose and release several pre-trained music representation networks, based on different learning strategies for multiple semantic learning tasks.

The global framework of our approach is illustrated in Fig. 2. The upper half of the scheme illustrates the procedure of *learning* a deep music representation; a formalization of this problem, as well as the global outline of how learning will be performed based on different learning tasks from different sources, will be presented in Section 2. Detailed specifications of the deep architectures we considered for the learning procedure (the representation network in Fig. 2) will be discussed in Section 3. Our strategy to *evaluate* the effectiveness of different representation network variants by employing various *evaluation tasks* is illustrated by the lower half of Fig. 2, and will be the focus of Section 4. Experimental results will be discussed in Section 5, after which general conclusions will be presented in Section 6.

## 2 Framework for Deep Representation Learning

In this section we formally define the deep representation learning problem. This considers the upper half of the scheme in Fig. 2, with the exception of details of the deep learning architecture itself, which will be discussed in Section 3.

## 2.1 Problem Definition

A machine learning problem, focused on solving a specific task  $t$ , can be formulated as a minimization problem, in which a model function  $f^t$  must be learned that minimizes a loss function  $\mathcal{L}$ , comparing the inferred model’s predictions and actual task-specific learning targets  $y^t$ . This can be formulated using the following expression:

$$\min_{\theta} \mathcal{L}(y^t, f^t(x; \theta)) \quad (1)$$

where  $x \in \mathbb{R}^d$  is, traditionally, a hand-crafted  $d$ -dimensional feature vector and  $\theta$  is a set of model parameters of  $f$ .

When deep learning is employed, the model function  $f$  denotes a learnable network. Typically, the network model  $f$  is learned in an end-to-end fashion, from raw data at the input to the learning target. In the speech and music field, however, using true end-to-end learning is still not a common practice. Instead, raw data is typically transformed first, before serving as network input. More specifically, in the music domain, common input to function  $f$  would be  $X \in \mathbb{R}^{c \times n \times b}$ , replacing the originally hand-crafted feature vector  $x \in \mathbb{R}^d$  from (1) by a time-frequency representation of the observed music data, usually obtained through the Short-Time Fourier Transform (STFT), with potential additional filter bank applications (e.g. Mel-filter bank). The dimensions  $c$ ,  $n$ ,  $b$  indicate channels of the audio signal, time steps, and frequency bins respectively.

If such a network still is trained for a specific single machine learning task  $t$ , we can now reformulate (1) as follows:

$$\min_{\theta} \mathcal{L}(y^t, f^t(X; \theta)). \quad (2)$$

In MTL, in the process of learning the network model  $f$ , different tasks will need to be solved in parallel. In case of deep neural networks, this is usually realized by having a network in which lower layers are shared for all tasks, but upper layers are task-specific. Given  $m$  different tasks  $t$ , each having the learning target  $y^t$ , we can formulate the learning objective of the neural network in a MTL scenario as follows:

$$\min_{\theta^*, \theta^s} \sum_{t \in T} \mathcal{L}(y^t, f^t(X; \theta^t, \theta^s)) \quad (3)$$

Here,  $T = \{t_1, t_2, \dots, t_m\}$  is a given set of tasks to be learned and  $\theta^* = \{\theta^1, \theta^2, \dots, \theta^m\}$  indicates a set of model parameters  $\theta^t$  with respect to each task. Since the deep architecture initially shares lower layers and branches out to task-specific upper layers, the parameters of shared layers and task-specific layers are referred to separately as  $\theta^t$  and  $\theta^s$ . Updates for all parameters can be achieved through standard back-propagation. Further specifics on network architectures and training configurations will be given in Section 3.

Given the formalizations above, the first step in our framework is to select a suitable set  $T$  of learning tasks. These tasks can be seen as multiple concurrent descriptions or transformations of the same input fragment of musical audio: each will reflect certain semantic aspects of the music. However, unlike the approach in a typical MTL scheme, solving multiple specific learning tasks is actually not our main goal; instead, we wish to learn an effective *representation* that captures as many semantically important factors in the low-level music representation. Thus, rather than using learning targets  $y^t$ , our representation learning process will employ reduced learning targets  $z^t$ , which capture a reduced set of semantic factors from  $y^t$ . We then can reformulate (3) as follows:

$$\min_{\theta^*, \theta^s} \sum_{t \in T} \mathcal{L}(z^t, f^t(X; \theta^t, \theta^s)) \quad (4)$$

where  $z^t \in \mathbb{R}^k$  is a  $k$ -dimensional reduced learning target for a specific task  $t$ . Each  $z^t$  will be obtained through task-specific factor extraction methods, as described in Section 2.3.

## 2.2 Learning Sources

So far, we discussed learning tasks and learning targets in the context of machine learning schemes. Conceptually, learning tasks can be seen as problems to be solved, while learning targets are ‘sample solutions’ to the problem, considering a given training dataset. We did not yet discuss who or what authored these ‘sample solutions’; in other words, we did not yet discuss the *learning sources*.

In fact, different learning sources of different nature can be imagined, that can be globally categorized as *Algorithm* or *Label*. As for the *Algorithm* category, by employing traditional feature extraction or representation transformation algorithms, we will be able to extract semantically interesting aspects from input data. As for the *Label* category, these include different types of semantic label annotations of the input data by humans.

The dataset used as resource for our learning experiments is the Million Song Dataset (MSD)[28]. In its original form, it contains metadata and precomputed features for a million songs, with several associated data resources, e.g. considering `Last.fm` social tags and listening profiles from `the Echo Nest`. While the MSD does not distribute audio due to copyright reasons, through the API of the `7digital` service, 30-second audio previews can be obtained for the songs in the dataset. These 30-second previews will form the source for our raw audio input.

Using the MSD data, we consider several subcategories of learning sources within the *Algorithm* and *Label* categories; below, we give an overview of these, and specify what information we considered exactly for the learning targets in our work.

### 2.2.1 Algorithm

- **Self.** The music track is the learning source itself; in other words, intrinsic information in the input music track should be captured through a learning procedure, without employing further data. Various unsupervised or auto-regressive learning strategies can be employed under this category, with variants of Autoencoders, including the Stacked Autoencoder [29, 30], Restricted Boltzmann Machines (RBM) [31], and Deep Belief Networks (DBN) [32]. Also, semi-supervised or supervised learning schemes can be used; here, Generative Adversarial Networks (GAN)[33] are a popular choice. As another example within this category, variants of the Siamese networks for similarity learning can be considered [34, 35, 36].

In our case, we will employ the Siamese architecture to learn a metric that measures whether two input music clips belong to the same track, or two different tracks. This can be formally formulated as follows:

$$\min_{\theta^{self}, \theta^s} \mathcal{L}(y^{self}, f^{self}(X_l, X_r; \theta^{self}, \theta^s)) \quad (5)$$

$$y^{self} = \begin{cases} 1, & \text{if } X_l \text{ and } X_r \text{ sampled from same track} \\ 0 & \text{otherwise} \end{cases} \quad (6)$$

where  $X_l$  and  $X_r$  are a pair of randomly sampled short music snippets (taken from the 30-second MSD audio previews) and  $f^{self}$  is a network for learning a metric between given input representations in terms of the criteria imposed by  $y^{self}$ . It is composed of one or more fully-connected layers and one output layer with softmax activation. An global outline illustration of our chosen architecture is given in Fig. 3. Further specifications of the representation network and sampling strategies will be given in Section 3.

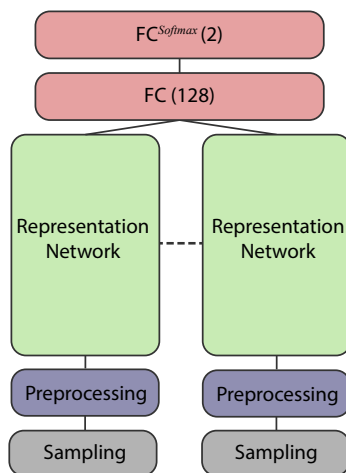


Fig. 3: Siamese architecture adopted for the *Self* learning task. For further details of the Feature Network, see Section 3.1 and Fig. 4.

- **Feature.** Many algorithms exist already for extracting features out of musical audio, or for transforming musical audio representations. By running such algorithms on musical audio, learning targets are automatically computed, without the need for soliciting human annotations. Algorithmically computed outcomes will likely not be perfect, and include noise or errors. At the same time, we consider them as a relatively efficient way to extract semantically relevant and more structured information out of a raw input signal.

In our case, under this category, we use BPM information, released as part of the MSD’s pre-computed features. The BPM values were computed by an estimation algorithm, as part of the Echo Nest API.

### 2.2.2 Label

- **Metadata.** Typically, metadata will come ‘for free’ with music audio, specifying side information, such as a release year, the song title, the name of the artist, the corresponding album name, and the corresponding album cover image. Considering that this information describes categorization facets of the musical audio, metadata can be a useful information source to learn a music representation. In our experiments, we use release year information, which is readily provided as metadata with each song in the MSD.

- **Crowd.** Through interaction with music streaming or scrobbling services, large numbers of users, also designated as the *crowd*, left explicit or implicit information regarding their perspectives on musical content. For example, they may have created social tags, ratings, or social media mentionings of songs. With many services offering API access to these types of descriptors, crowd data therefore offers scalable, spontaneous and diverse (albeit noisy) human perspectives on music signals.

In our experiments, we use social tags from `Last.fm`<sup>1</sup> and user listening profile from the `Echo Nest`.

- **Professional.** As mentioned in [1], annotation of music tracks is a complicated and time-consuming process: annotation criteria frequently are subjective, and considerable domain knowledge and annotation experience may be required before accurate and consistent annotations can be made. Professional experts in categorization have this experience, and thus are capable of indicating clean and systematic information about musical content. It is not trivial to get such professional annotations at scale; however, these types of annotations may be available in existing professional libraries.

In our case, we use professional annotations from the Centrale Discotheek Rotterdam (CDR), the largest music library in The Netherlands, holding all music ever released in the country in physical and digital form in its collection. The CDR collection can be digitally accessed through the online Muziekweb<sup>2</sup> platform. For each musical album in the CDR collection, genre annotations were made by a professional annotator, according to a fixed vocabulary of 367 hierarchical music genres.

As another professional-level ‘description’, we adopted lyrics information per each track, which is provided in Bag-of-Words format with the MSD. To filter out trivial terms such as stop-words, we applied TF-IDF[37].

- **Combination.** Finally, learning targets can be derived from combinations of the above categories. In our experiment, we used combination of artist information and social tags, by making a bag of tags at the artist level as a learning target.

Not all songs in the MSD actually include learning targets from all the sources mentioned above. For our experiment, we chose to only focus on that subset of the dataset for which this was the case. As a consequence, we managed to collect 46,490 clips of tracks with corresponding learning task targets. A 41,841 / 4,649 split was made for training and validation. Since we mainly focus on transfer learning, we used the validation set mostly for monitoring the training, to keep the network from overfitting.

### 2.3 Latent Factor Preprocessing

Most learning sources are noisy. For instance, social tags include tags for personal playlist management, long sentences, or simply typos, which do not actually show relevant nuances in describing the music signal. The algorithmically extracted BPM information also is imperfect, and likely contains octave errors, in which BPM is under- or overestimated by a factor of 2. To deal with this noise, several previous works using the MSD [5, 13] applied a frequency-based filtering strategy along with top-down domain knowledge. However, this shrinks the available sample size. As an alternative way

<sup>1</sup> <https://labrosa.ee.columbia.edu/millionsong/lastfm>

<sup>2</sup> <https://www.muziekweb.nl/>



Table 1: Properties of learning sources.

Identifier	Category	Data	Dimensionality	Preprocessing	
<i>self</i> <i>bpm</i>	Algorithm	Self	MSD - Track	1	
		Feature	MSD - BPM	1	GMM
<i>year</i>		Metadata	MSD - Year	1	GMM
<i>tag</i>		Crowd	MSD - Tag	174,156	pLSA
<i>taste</i>	Label	Crowd	MSD - Taste	949,813	pLSA
<i>cdr_tag</i>		Professional	CDR - Tag	367	pLSA
<i>lyrics</i>		Professional	MSD - Lyrics	5,000	pLSA, TF-IDF
<i>artist</i>		Combination	MSD - Artist & Tag	522,366	pLSA

Table 2: Examples of Latent Topics extracted with pLSA from MSD social tags

Topic	Strongest social tags
tag1	indie rock, indie, british, Scottish
tag2	pop, pop rock, dance, male vocalists
tag3	soul, rnb, funk, Neo-Soul
tag4	Melodic Death Metal, black metal, doom metal, Gothic Metal
tag5	fun, catchy, happy, Favorite

to handle noisiness, several other previous works [6, 14, 38, 39, 40, 41] apply latent factor extraction using various low-rank approximation models to preprocess the target information. We also choose to do this in our experiments.

A full overview of chosen learning sources, their category, origin dataset, dimensionality and preprocessing strategies is shown in Table 1. In most cases, we apply probabilistic latent semantic analysis (pLSA), which extracts latent factors as a multinomial distribution of latent topics [42]. Table 2 illustrates several examples of strong social tags within extracted latent topics. For situations in which learning targets are a scalar, non-binary value (BPM and release year), we applied a Gaussian Mixture Model (GMM) to transform each value into a categorical distribution of Gaussian components. In case of the *Self* category, as it basically is a binary membership test, no factor extraction was needed in this case.

After preprocessing, learning task targets  $y^t$  are now expressed in the form of probabilistic distributions  $z^t$ . Then, the learning of a deep representation can take place by minimizing the Kullback–Leibler (KL) divergence between model inferences  $f^t(X)$  and target factor distributions  $z^t$ . For a clearer comparison between tasks and for simplicity, we used a fixed single value  $k = 50$  for the number of factors (pLSA) and the number of Gaussians (GMM).

### 3 Representation Network Architectures

In this section, we present the detailed specification of the deep representation neural network architecture we exploited in this work. This part corresponds to the representation network in Fig. 2. We will discuss base architecture of the network, and further discuss the shared architecture with respect to different fusion strategies that one can take in the MTDTL context. Also, we introduce details on the pre-processing related to the input data served into networks.

### 3.1 Base Architecture

As deep base architecture for feature representation training and learning, we choose a Convolutional Neural Network (CNN) architecture inspired by [8], as illustrated in Fig. 4.

The CNN is one of the most popular architectures in many music-related machine learning tasks [5, 6, 43, 44]. Many of these works adopt an architecture having cascading blocks of 2-dimensional filters and max-pooling, derived from well-known works in image recognition [8, 45]. Although variants of CNN using 1-dimensional filters also were suggested by [23, 27, 46, 47] to learn features directly from a raw audio signal in an end-to-end manner, not many works managed to use them on music classification tasks successfully [48].

We applied the Rectified Linear Unit (ReLU) [49] to all convolution layers and the **fc-feature** layer. For the **fc-output** layer, softmax activation is used. To accelerate the training and stabilize the internal covariance shift [50], we also apply Batch-Normalization (BN) for every convolution layer and the **fc-feature** layer. As for the regularization, we choose to apply drop-out [51] on the **fc-feature** layer. We added  $L2$  regularization across all the parameters with the same weight  $\lambda = 1e - 6$ . Further details of the base architecture are summarized in Table 3.

#### 3.1.1 Audio Preprocessing

We aim to learn a music representation from as-raw-as-possible input data to fully leverage the capability of the neural network. For this purpose, we use the dB-scale Mel-scale magnitude spectrum of an input audio fragment, extracted by applying 128-band Mel-filter banks on the Short-Time Fourier Transform (STFT). Mel-Spectrograms have generally been a popular input representation choice for CNNs applied in music-related tasks [5, 6, 13, 40, 43, 52]; besides, it also was reported recently that their frequency-domain summarization, based on psycho-acoustics, is efficient and not easily learnable through data-driven approaches [53, 54]. We choose a 1024-sample window size and 256-sample hop size, translating to about 46 ms and 11.6 ms respectively for a sampling rate of 22 kHz. We also applied standardization to each Mel spectrum, making use of the mean and variance of all individual Mel spectra in the training set.

#### 3.1.2 Sampling

During the learning process, in each iteration, a random batch of songs is selected. Audio corresponding to these songs originally is 30 seconds in length; for data augmentation and computational efficiency, we randomly crop 2.5 seconds out of each song each time. Keeping stereo channels of the audio, the size of a single input tensor we used for the experiment ended up with  $2 \times 216 \times 128$ , where the first dimension indicates number of channels, and following dimensions mean time steps and Mel-bins, respectively. For the *Self* case, we generate batches with equal numbers of songs for both membership categories in  $y^{Self}$ .

### 3.2 Multi-Task Architectures with Various Degrees of Shared Information

When learning a music representation based on various available learning sources, different strategies can be taken regarding the choice of architecture. We will investigate the following setups:

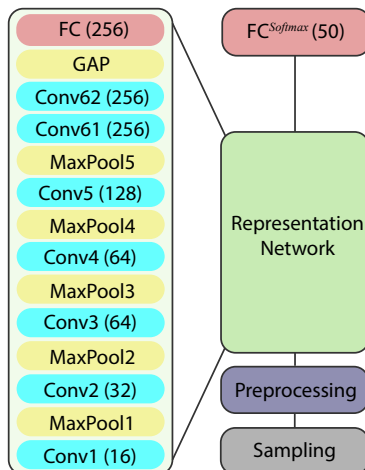


Fig. 4: Default CNN architecture for supervised single-task representation learning. Details of the Feature Network are presented at the left of the global architecture diagram. The numbers inside the parentheses indicate either the number of filters or the number of units with respect to the type of layer.

Table 3: Configuration of the base CNN. `conv` and `max-pool` indicate a 2-dimensional convolution and max-pooling layer, respectively. We set the stride size with 2 on the time dimension of `conv1`, to compress dimensionality at the early stage. Otherwise, all strides are set as 1 across all the convolution layers. `gap` corresponds to the global average pooling used in [55], which averages out all the spatial dimensions of the filter responses. `fc` is an abbreviation of fully-connected layer. We use `dropout` with  $p = 0.5$  only for the `fc-feature` layer, where the intermediate latent representation is extracted and evaluated. For simplicity, we omit the batch-size dimension of the input shape.

Layer	Input Shape	Weight Shape	Sub-sampling	Activation
<code>conv1</code>	$2 \times 216 \times 128$	$2 \times 16 \times 5 \times 5$	$2 \times 1$	ReLU
<code>max-pool1</code>	$16 \times 108 \times 128$		$2 \times 2$	
<code>conv2</code>	$16 \times 54 \times 64$	$16 \times 32 \times 3 \times 3$		ReLU
<code>max-pool2</code>	$32 \times 54 \times 64$		$2 \times 2$	
<code>conv3</code>	$32 \times 27 \times 32$	$32 \times 64 \times 3 \times 3$		ReLU
<code>max-pool3</code>	$64 \times 27 \times 32$		$2 \times 2$	
<code>conv4</code>	$64 \times 13 \times 16$	$64 \times 64 \times 3 \times 3$		ReLU
<code>max-pool4</code>	$64 \times 13 \times 16$		$2 \times 2$	
<code>conv5</code>	$64 \times 6 \times 8$	$64 \times 128 \times 3 \times 3$		ReLU
<code>max-pool5</code>	$128 \times 6 \times 8$		$2 \times 2$	
<code>conv61</code>	$128 \times 3 \times 4$	$128 \times 256 \times 3 \times 3$		ReLU
<code>conv62</code>	$256 \times 3 \times 4$	$256 \times 256 \times 1 \times 1$		ReLU
<code>gap</code>	256			
<code>fc-feature</code>	256	$256 \times 256$		ReLU
<code>dropout</code>	256			
<code>fc-output</code>	256	task specific		Softmax

Table 4: Properties of the various categories of representation learning architectures.

	Multi Task	Shared Network	Concatenation	Dimensionality
<b>SS-R</b>	No	No	No	$d$
<b>MSS-CR</b>	Yes	No	Yes	$d \times m$
<b>MS-CR</b>	Yes	Partial	Yes	$d \times m$
<b>MS-SR</b>	Yes	Yes	No	$d$

- As a base case, a **Single-Source Representation (SS-R)** representation can be learned for a single task only. As mentioned earlier, this would be the typical strategy leading to pre-trained networks, that later would be used in transfer learning. In our case, our base architecture from Section 3.1 and Fig. 4 will be used, for which the layers in the Feature Network also are illustrated in Fig. 5a. Out of the **fc-feature** layer, a  $d$ -dimensional representation is obtained.
- If multiple perspectives on the same content, as reflected by the multiple learning targets, should also be reflected in the ultimate learned representation, one can learn *SS-R* representations for each learning source, and simply concatenate them afterwards. With  $d$  dimensions per task and  $m$  tasks, this leads to a  $d \times m$  **Multiple Single-Source Concatenated Representation (MSS-CR)**. In this case, independent networks are trained for each of the tasks, and no shared knowledge will be transferred between tasks. A layer setup of the corresponding Feature Network is illustrated in Fig. 5b.
- When applying MTL learning strategies, the deep architecture should involve shared knowledge layers, before branching out to various individual learning sources, whose learned representations will be concatenated in the final  $d \times m$ -dimensional representation. We call these **Multi-Source Concatenated Representations (MS-CR)**. As the branching point can be chosen at different stages, we will investigate the effect of various prototypical branching point choices: at the second convolution layer (*MS-CR@2*, Fig. 5c), the fourth convolution layer (*MS-CR@4*, Fig. 5d), and the sixth convolution layer (*MS-CR@6*, Fig. 5e). The later the branching point occurs, the more shared knowledge the network will employ.
- In the most extreme case, branching would only occur at the very last fully connected layer, and a **Multi-Source Shared Representation (MS-SR)** (or, more specifically, *MS-SR@FC*) is learned, as illustrated in Fig. 5f. As the representation is obtained from the **fc-feature** layer, no concatenation takes place here, and a  $d$ -dimensional representation is obtained.

A summary of these different representation learning architectures is given in Table 4. Beyond the strategies we choose, further approaches can be thought of to connect representations learned for different tasks in neural network architectures. For example, for different tasks, representations can be extracted from different intermediate hidden layers, benefiting from the hierarchical feature encoding capability of the deep network [13]. However, considering that learned representations are usually taken from a specific fixed layer of the shared architecture, we focus on the strategies as we outlined above.

### 3.3 MTL Training Procedure

Similar to [17, 39], we choose to train the MTL models with a stochastic update scheme as described in Algorithm 1. At every iteration, a task is selected randomly. After the task is chosen, a batch

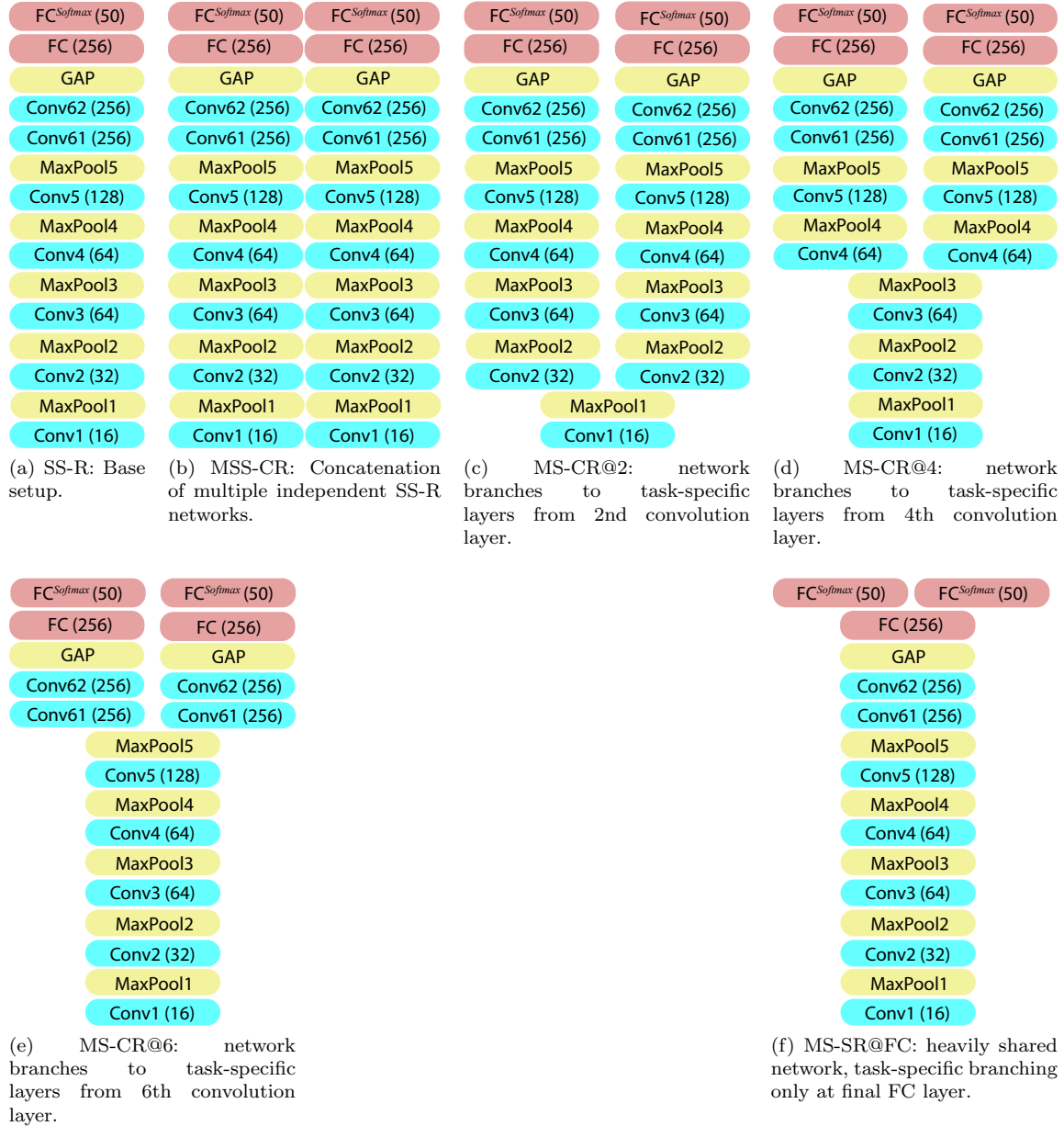


Fig. 5: The various model architectures considered in the current work. Beyond single-task architectures, multi-task architectures with various degrees of shared information are studied. For simplification, multi-task cases are illustrated here for two tasks. The **fc-feature** layer from which representations will be extracted is the FC(256) layer in the illustrations (see Table 3).

**Algorithm 1:** Training a Multi-task CNN

---

```

1 Initialize  $\Theta: \{\theta^t, \theta^s\}$  randomly;
2 for epoch in  $1 \dots N$  do
3   for iteration in  $1 \dots L$  do
4     Pick a task  $t$  randomly;
5     Pick batch of samples from task  $t$ ;
6      $(X_l, X_r)$  for Self;
7      $X$  otherwise;
8     Derive learning target  $z^t$ ;
9     Sub-sample chunk  $X^*$  from track  $X$ ;
10    Forward-pass;
11     $\mathcal{L}(y^{Self}, \Theta, X_l^*, X_r^*) = \text{Eq. 5}$  for Self;
12     $\mathcal{L}(z^t, \Theta, X^*) = \text{Eq. 2}$  otherwise;
13    Backward-pass:  $\nabla(\Theta)$ ;
14    Update model:  $\Theta \leftarrow \Theta - \epsilon \nabla(\Theta)$ ;

```

---

of observation-target pairs  $(X, z^t)$  are drawn. For the audio previews belonging to the songs within this batch, an input representation  $X^*$  is cropped randomly from its super-sample  $X$ . The updates of the parameters  $\Theta$  are conducted through back-propagation using the Adam algorithm[56]. For each neural network we train, we set  $L = l \times m$ , where  $l$  is the number of iterations needed to visit all the training samples with fixed batch size  $b = 48$ , and  $m$  is the number of learning sources used in the training. Across the training, we used a fixed learning rate  $\epsilon = 0.0001$ . After a fixed number of epochs  $N$  is reached, we stop the training.

### 3.4 Implementation Details

We used *Lasagne* [57] and *Theano* [58] to implement the CNN models and used *Fuel* [59] for parallel data serving. For evaluation models and cross-validation, we made extensive use of functionality in *Scikit-Learn* [60]. Furthermore, *Librosa* [61] was used to process audio files. As will be explained in Section 4, CNN training was performed for 90 experimental runs; in each run, for a given combination of learning sources, training was performed for a given deep architecture. This training procedure took approximately 3 weeks with 5 Graphical Processing Unit (GPU) computation nodes, composed of 4 NVIDIA GRID K2 GPUs and one NVIDIA GTX 1070 GPU.

## 4 Evaluation

In this section, we present the evaluation strategy for our experiments. This corresponds to the lower half of Fig. 2. At first, we will introduce the experimental design in Section 4.1, after which we will discuss chosen evaluation tasks and datasets in Section 4.2. We then discuss the implementation of our evaluation experiments in Section 4.3). Finally, we discuss the baselines against which our representations will be compared in Section 4.4.

#### 4.1 Experimental Design

In order to investigate **RQ1** and **RQ2**, we carried out an experiment to study the effect of the number and type of learning sources on the effectiveness of deep representations, as well as the effect of the various architectural learning strategies described in Section 3.2. For the experimental design we consider the architecture factor (6-level factor, namely *SS-R*, *MSS-CR*, *MS-CR@2*, *MS-CR@4*, *MS-CR@6*, and *MS-SR@FC*), and 8 2-level factors, indicating binary membership of each of the 8 learning sources (see Table 1) in the set of learning tasks  $T$  feeding into the deep architecture. However, and given the constraint of *SS-R* relying on a single learning source, we proceeded in two steps.

In the first step, we produce a design for *MS-SR@FC* and the 3 *MS-CR* strategies (in other words, 4 different choices of architecture). Together with the 8 learning sources, a full factorial design would require 1,024 runs, which unfortunately was infeasible to exhaustively run, given available resources. To our knowledge though, there is no standard fractional design of these characteristics, so we proceeded to make an optional design that would allow us to study main effects while minimizing confounding with two-factor interactions, minimizing the required number of runs, and maintaining desired orthogonality and balance properties [62]. The final design consists of 78 runs from the optimal design, plus the additional run with  $|T| = 8$  for each of *MS-SR@FC* and the 3 *MS-CR* strategies, leading to a total of 82 different representation networks to be trained. This design produces virtually no confounding between main effects.

In the second step, we first trained 8 representation networks independently, following the *SS-R* strategy. The only strategy not yet discussed at this stage is *MSS-CR*, which concatenates representations from multiple *SS-R* networks. As a consequence, these representations can be gained ‘for free’ without having to retrain a representation network. We considered *MSS-CR* representations for each combination of tasks reflected in our 78 experimental combinations from the first step, as well as for the case in which all 8 *SS-R* representations would be concatenated.

Thus, we trained  $82 + 8 = 90$  representation networks in total, and from these networks, we could extract  $90 + 78 + 1 = 169$  different deep music representations.

Each considered representation network was trained using the CNN representation network model from Section 3, based on the specific combination of learning sources and deep architecture as indicated by the experimental run. In order to reduce variance, we fixed the number of training epochs to  $N = 100$  across all runs, and applied the same base architecture, except for the branching point.

All representations were validated in the context of various evaluation datasets with corresponding evaluation tasks, as detailed in the following section.

#### 4.2 Evaluation Tasks and Datasets

In order to give insight into the effectiveness of learned representations with respect to multiple potential unseen tasks, we consider a range of *evaluation tasks*, exemplified by several datasets carefully chosen so as to reflect various semantic properties of music, purposefully chosen semantic biases, or popularity in the MIR literature. This evaluation data should not have been seen by the representation network during its training, nor should the representation network have been configured to explicitly solve the chosen evaluation tasks.

While for the learning sources, we could provide categorizations on where and how the learning targets were derived, and also consider algorithmical outcomes as targets, existing popular research

datasets mostly fall in the *Professional* or *Crowd* categories. To seek a more reliable result, we chose 7 evaluation datasets commonly used in MIR research, which reflect three conventional types of MIR evaluation task, namely classification, regression and recommendation:

- **Classification.** Different types of classification tasks exist in MIR: in our experiments, we consider several datasets used for genre classification and instrument classification.

As for genre classification, we chose the GTZAN [63] and FMA [64] datasets as main exemplars. Even though GTZAN is known for its caveats [65], we deliberately used it because its popularity can be beneficial when comparing with previous and future work. We note though that there may be some overlap between the tracks of GTZAN and the subset of the MSD we use in our experiments; the extent of this overlap is unknown, due to the lack of a confirmed and exhaustive track listing of the GTZAN dataset.

Among the various packages provided by the FMA, we chose the top-genre classification task of FMA-Medium [64]. This is a classification task with unbalanced genre distribution. We sub-sampled 5% of the entire dataset for computationally efficient evaluation.

Considering another type of genre classification, we selected the Ballroom dataset [66]. Because the classes in this dataset are highly separable with regard to their BPM [67], we specifically included this ‘purposefully biased’ task as an example of how a learned representation may effectively capture temporal dynamics properties present in an evaluation task, as long as learning sources also reflected these properties.

The last dataset we considered for classification is the training set of the IRMAS dataset [68], which consists of short music clips annotated with the predominant instruments present in the clip. Compared to the genre classification task, instrument classification is generally considered as less subjective, requiring features to separate timbral characteristics of the music signal as opposed to high-level semantics like genre. For efficiency purposes, we similarly sub-sampled 20% of this dataset.

As performance metric for all these classification tasks, we used classification accuracy.

- **Regression.** As exemplars of regression tasks, we evaluate our proposed deep representations on the dataset used in the MediaEval Music Emotion prediction task [69]. It contains frame-level and song-level labels of a two-dimensional representation of emotion, with valence and arousal as dimensions [70]. Valence is related to the positivity or negativity of the emotion, and arousal is related to its intensity [69]. The song-level annotation of the V-A coordinates was used as the learning target, and we trained separate models for the two emotional dimensions.

As evaluation metric, we measured the coefficient of determination ( $R^2$ ) of each model.

- **Recommendation.** Finally, we employed the ‘This Is My Jam’ dataset [71] to evaluate our deep representations in the context of a content-aware music recommendation task. In this dataset, users posted a ‘jam’ (their favorite song at a certain time), which could yield *Likes*, indicating other users’ binary preference on the jams. Furthermore, information is available on *Followers*, offering mappings between different users. In our case, we use *Likes* information to predict which jam is most likely preferred by users, and base our deep music content representations on the MSD-matched audio previews for a jam.

In our experiments, we mimicked a cold-start recommendation problem, in which items not seen before should be recommended to the right users. For efficiency, we sub-sampled the dataset to contain 944 unique tracks and 993 users.

Similar to [72], we considered *outer matrix* performance for un-introduced songs; in other words, the model’s recommendation accuracy on the items newly introduced to the system[72]. This was done by holding out certain tracks when learning user models, and then predicting user



Table 5: Properties of evaluation tasks. Datasets with asterisk indicate that we uniformly sampled them from original dataset for time efficiency. The original numbers of the samples are placed in the parenthesis.

Task	Data		#Observation	#Class
Classification	FMA*[64]	Genre	1,250 (25,000)	16
Classification	GTZAN[63]	Genre	1,000	10
Classification	Ballroom[66]	Genre	698	10
Classification	IRMAS*[68]	Instrument	1,341 (6,705)	11
Regression	Music Emotion[69]	Arousal	744	
Regression	Music Emotion[69]	Valence	744	
Recommendation	ThisIsMyJam*[71]	Likes	944 (533,266)	

preference scores based on all tracks, including those that were held out, resulting in a ranked track list per user. As evaluation metric, we then consider Average Precision (AP)@20, only treating held-out tracks that were indeed liked by a user as relevant items. Further details on how hold-out tracks were chosen are given in the following section.

A summarization of all evaluation datasets, their origins and their properties can be found in Table 5.

### 4.3 Evaluation Implementation

In order to assess how our learned deep music representations perform on the various evaluation tasks, transfer learning will now be applied, to consider our representations in the context of these new and unseen tasks.

As a consequence, new machine learning pipelines are set up, focused on each of the evaluation tasks. In all cases, we randomly split the dataset in a 90% training and 10% test set, repeating 50 times. In most of our evaluation cases, validation will take place on the test set; in case of the the recommendation problem, the test set represents a set of tracks to be held out during user model training, and re-inserted for validation. In all cases, we will extract representations from evaluation dataset audio as detailed in Section 4.3.1, and then learn relatively simple models based on them, as detailed in Section 4.3.2. Employing the metrics as mentioned in the previous section, we will then take average performance scores over the 50 different train-test splits for final performance reporting.

#### 4.3.1 Feature Extraction and Preprocessing

Taking raw audio from the evaluation datasets as input, we take non-overlapping slices out of this audio with a fixed length of 2.5 seconds. Based on this, we apply the same preprocessing transformations as discussed in Section 3.1.1. Then, we extract a deep representation from this preprocessed audio, employing the architecture as specified by the given experimental run. As in the case of Section 3.2, representations are extracted from the **fc-feature** layer of each trained CNN model. Depending on the choice of architecture, the final representation may consist of concatenations of representations obtained by separate representation networks.

Input audio may originally be (much) longer than 2.5 seconds; therefore, we aggregate information in feature vectors over multiple time slices by taking their *mean* and *standard deviation* values. As a result, we get a representation with averages per learned feature dimension, and another representation with standard deviations per feature dimension. These will be concatenated, as illustrated in Fig. 2.

#### 4.3.2 Evaluation Task-Specific Models

To evaluate the trained representations, we used different models according to the target evaluation task. For classification and regression tasks, we used Support Vector Machines (SVM) [73, 74, 75].

As our goal is not to over-optimize task-specific performance, but rather perform a comparative analysis between different representations (resulting from different learning strategies), we keep the model simple, and use fixed hyper-parameter values for each model across the entire experiment. More specifically, the hyper-parameters of the SVM classifiers are set to  $C = 1$ , using a linear kernel. For SVM regressors, we used the same value for  $C$ , while we used a Radial Basis Function (RBF) kernel and the kernel parameter  $\gamma = 1/d$ , where  $d$  is the number of feature dimensions.

For the recommendation task, we choose a model suggested in [72], in which the learning objective function  $\mathcal{L}$  is defined as

$$\min_{U,V,W} \|R - UV^T\|_F + \frac{\lambda^V}{2} \|V - XW\|_2 + \frac{\lambda^U}{2} \|U\|_2 + \frac{\lambda^W}{2} \|W\|_2 \quad (7)$$

where  $R \in \mathbb{R}^{u \times i}$  is an input interaction matrix between  $u$  users and  $i$  items,  $U \in \mathbb{R}^{u \times r}$  and  $V \in \mathbb{R}^{i \times r}$  are  $r$  dimensional user factors and item factors for the low-rank approximation of  $R$ .  $W \in \mathbb{R}^{d \times r}$  is a free parameter for the projection from  $d$ -dimensional feature space to the factor space.  $X \in \mathbb{R}^{i \times d}$  is the feature matrix where each row corresponds to a track.

As for hyper-parameters, we set  $\lambda^V = 100$ ,  $\lambda^U = 1$ , and  $\lambda^W = 1$ , respectively. For the number of factors we choose  $r = 10$  to focus only on the relative impact of the representation over the different conditions. We implemented an update rule with the Alternating Least Squares (ALS) algorithm similar to [72], and updated parameters during 40 iterations.

#### 4.4 Baselines

We also examined a number of baselines to compare with our proposed representations:

- **Mel-Frequency Cepstral Coefficients (MFCC)**. These are some of the most popular audio representations in MIR research. In this work, we extract and aggregate MFCC following the strategy in [13]. In particular, we extracted 20 coefficients and also used their first- and second-order derivatives. After obtaining the time-frequency matrix and its derivatives, we performed aggregation by taking the average and standard deviation over the time dimension, resulting in a 120-dimensional vector representation.
- **Random Network Feature (Rand)**. We extracted the representation at the **fc-feature** layer without any representation network training. With random initialization, this representation therefore gives a random baseline for a given CNN architecture. We refer to this baseline as *Rand*.

- ***Latent Representation from Music Auto-Tagger (Choi)***. The work in [13], focused on a music auto-tagging task, can be considered as a state-of-the-art deep music representation for MIR. While the model’s focus on learning a representation for music auto-tagging can be considered as our *SS-R* case, there are a number of issues that complicate direct comparisons between this work and our work. First, the network in [13] is trained with about 4 times more data samples than in our experiments. Second, it employed a much smaller network than our architecture. Further, intermediate representations were extracted, which is out of the scope of our work, as we only consider representations at the **fc-feature** layer. Nevertheless, despite these caveats, the work still is very much in line with ours, making it a clear candidate for comparison. Throughout the evaluation, we could not fully reproduce the performance reported in the original paper [13]. When reporting our results, we therefore will report both the performance we obtained with the published model, referring to this as *Choi*, and the one reported in the original paper, referred to as *Choi paper*.

## 5 Results and Discussion

In this section, we present performances and discussions related to the proposed deep music representation with regard to each evaluation tasks. In Section 5.1, we will first compare the performance across the *SS-Rs*, to show how different individual learning sources work for each evaluation task. In Section 5.2, we will then present general experimental results related to the performance of the representations based on multiple learning sources at once. In Section 5.2.1, we discuss the effect of the number of learning sources exploited in the representation learning, in terms of the general performance, reliability, and model compactness. In Section 5.3, we discuss effectiveness of MT-DTL compared to DTL in MIR. Finally, we present some initial evidence for multifaceted semantic explainability of the proposed MTDTL in Section 5.4.<sup>3</sup>

### 5.1 Single-Source Representations

Fig. 6 presents the performance of *SS-R* on each of the 7 evaluation datasets. We can see that sources from the categories *Crowd*, *Professional* and *Combination* (i.e. *tag*, *taste*, *cdr\_tag*, *lyrics* and *artist*) always perform better than the *Rand* baseline. Compared to the *MFCC* baseline, representations learned from these single learning sources tend to perform better too, with the exceptions of the IRMAS and EmotionAro datasets, where *MFCC* outperforms most representations

On the other hand, we find that the *SS-Rs* from the other categories (i.e. *self*, *year* and *bpm*) tend to not perform better than the *Rand* baseline. Finally, *Choi*, the most sophisticated baseline we considered, generally performs at least as well as our best *SS-R*.

Zooming in to dataset-specific observed trends, the *bpm* learning source shows highly skewed performance across evaluation tasks: it clearly outperforms all other learning sources in the Ballroom dataset, achieving 88.37% of accuracy, but it achieves the worst performance in 4 other datasets. As shown in [67], this confirms that the Ballroom dataset is well-separable based on BPM information alone. Indeed, the representation trained on the *bpm* learning source seems to contain a latent representation close to the BPM of an input music signal. In contrast, we can see that the *bpm*

<sup>3</sup> For the reproductivity, we release all relevant materials including code, models, extracted features at <https://github.com/eldrin/MTLMusicRepresentation>

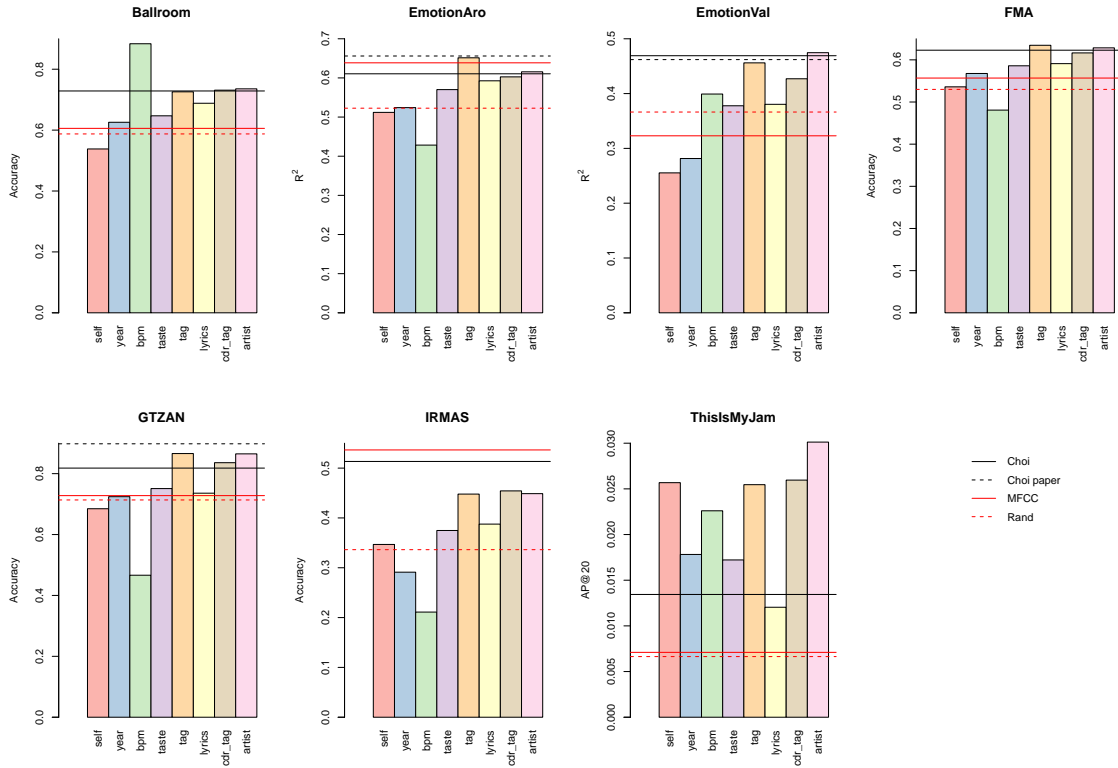


Fig. 6: Single task representation performance. Each bar indicates the average performance of the representation learned from each single source. The baselines are illustrated as horizontal lines.

representation achieves the worst results in the EmotionAro dataset, where both temporal dynamics and BPM are considered as important factors determining the intensity of emotion.

With respect to the ThisIsMyJam dataset, we notice that the *self* representation achieves the second-best performance, as opposed to the general trend found across the other datasets. [76] suggests that similarity-based side information performs well in recommendation settings because it can leverage similarities among music tracks, which may explain the good performance of this representation in this particular case.

On the IRMAS dataset, we see that all the *SS-Rs* perform worse than the *MFCC* and *Choi* baselines. Given that they both take into account low-level features, either by design or by exploiting low-level layers of the neural network, this suggests that predominant instrument sounds are harder to distinguish based solely on semantic features, which is the case of the proposed representations.

## 5.2 Multi-Source Representations

We now consider how the various representations based on multiple learning sources perform, in comparison to those based on single learning sources. The boxplots in Fig. 7 show the distributions

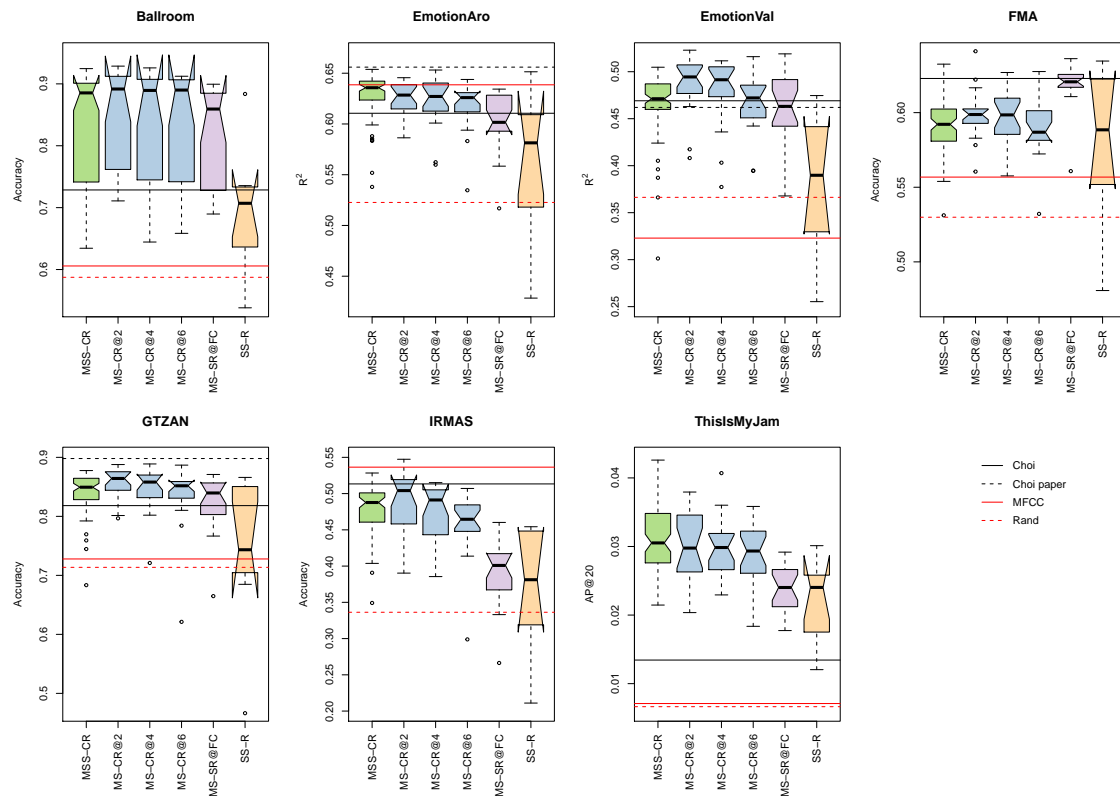


Fig. 7: Overall performance, considering different representation learning strategies.

of performance scores for each architectural strategy and per evaluation dataset. For comparison, the orange boxes summarize the distributions depicted in Fig. 6, based on the *SS-R* representations. In all datasets, we can see that the *SS-R* strategy obtains the lowest scores, followed by *MS-SR@FC*. Given that these representations have the same dimensionality, this results suggest that adding a single task-specific layer on top of a heavily shared model can help improving the adaptability of the neural network models.

The *MS-CR* and *MSS-CR* representations obtain the best results in general, with *MS-CR@2* and *MSS-CR* alternating as the best strategy per task. This is somewhat expected because of their larger dimensionality, but that might also lead to overfitting. This may be the reason why for the FMA dataset, we can see that the simplest *SS-R* strategies show similar performance to the more complex representations, which may have overfitted due to their large feature dimension. Still, the high performance of *MS-SR@FC* on this task shows that multiple learning sources, with a fixed-length representation, can still help separating the class space.

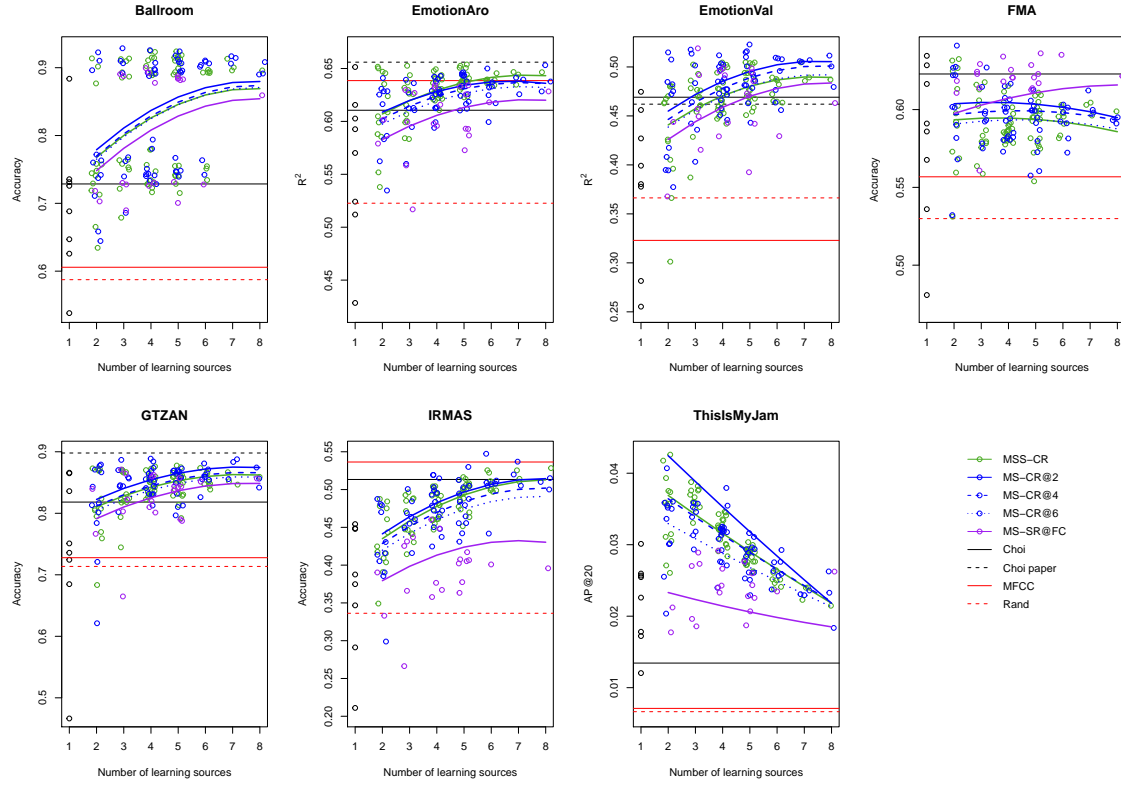


Fig. 8: Performance by number of learning sources, for each dataset and architecture strategy. The black circles at  $x = 1$  mark the performance of the 8 *SS-R* representations.

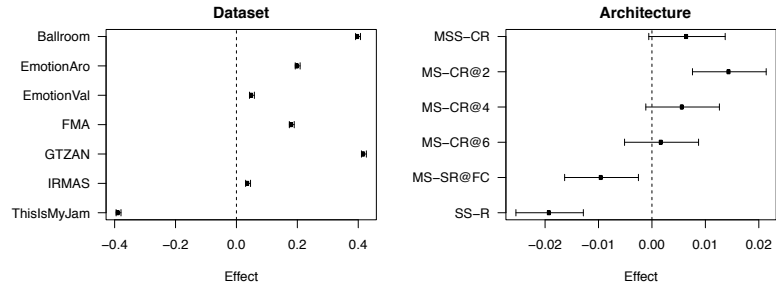


Fig. 9: Estimated effects and 95% confidence intervals for dataset and architecture effects.

### 5.2.1 Effect of Number of Learning Sources and Fusion Strategy

While the plots in Fig. 7 suggest that *MSS-CR* and *MS-CR* are the best strategies, the high observed variability makes this statement still rather inconclusive. In order to gain better insight into the effects of dataset, architecture strategies and number and type of learning sources, we fitted a hierarchical or multilevel linear model on all observed scores [77]. After model simplifications, in the end we allowed for random intercepts and slope of the number of learning sources within datasets, strategies and their interaction.

According to this model, there is a positive overall effect of the number of learning sources. There are significant variations across datasets, but not across architecture strategies. This means that, generally speaking, using more sources leads to better results, and the magnitude of this improvement depends on the specific evaluation dataset at hand, though not apparently so on the specific architecture strategy. Fig. 8 depicts all the observed performance scores. In the case of the Ballroom dataset, as clearly indicated by the bimodal distribution of results, whether the *bpm* learning source is included or not has a great impact on the performance. Also, note that as the number of sources increases, so does the likelihood that *bpm* will be included in the set of learning sources in the first place. In the case of ThisIsMyJam, there is a negative effect of the number of sources, which may be explained by the particular task-specific model we used for this dataset. With its maximum margin property, SVM can be effective to handle high-dimensional input, but the model we employed in Eq. 7 can be less robust in terms of regularization.

In terms of intercepts, we can see very large differences across datasets (see Fig. 9). These differences are expected because datasets are inherently different in terms of difficulty, and they are also evaluated with different evaluation metrics. As for the different architecture strategies, we can see smaller effects in comparison to datasets. Even so, Fig. 9 indicates there is a clear, yet non-significant pattern among fusion strategies. Confirming our previous observations, *SS-R* and *MS-SR@FC* perform significantly worse than the rest. In terms of the *MS-CR* variants, we can identify a trend with respect to the branch point, and as suggested above, *MSS-CR*, which employs concatenation of individually trained representations, performs similarly to representations trained from multiple sources at once.

### 5.2.2 Reliability

Fig. 8 also suggests that the variability of performance scores decreases with the number of learning sources used. Specifically, in Fig. 10, we plot the standard deviation of scores as a function of the number of learning sources, showing a clearly decreasing trend. This implies that if there are more learning sources available, one can expect more reliable performance from the learned representation. Most importantly, variability obtained for a single learning source ( $x = 1$ ) is always larger than the variability with 2 or more sources. Again, the Ballroom dataset shows much smaller variability when BPM is included in the combination. For this specific dataset, this indicates that once *bpm* is used to learn the representation, the expected performance is stable and does not vary much, even if we keep including more sources.

### 5.2.3 Compactness

Under an MTDTL setup with branching (the *MS-CR* architectures), as more learning sources are used, not only the representation will grow larger, but so will the necessary deep network to learn it:

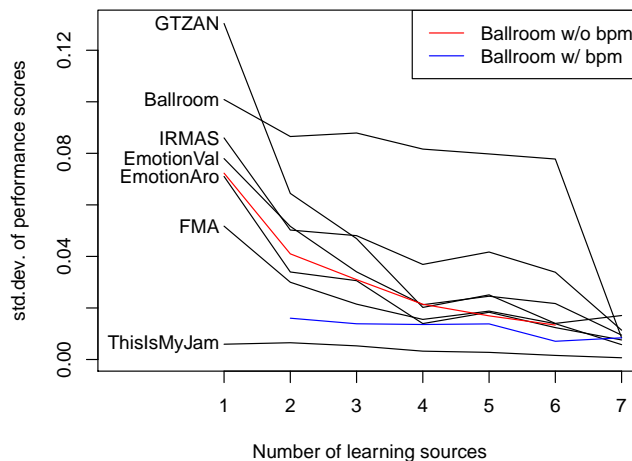


Fig. 10: Standard deviation of performance by number of learning sources.

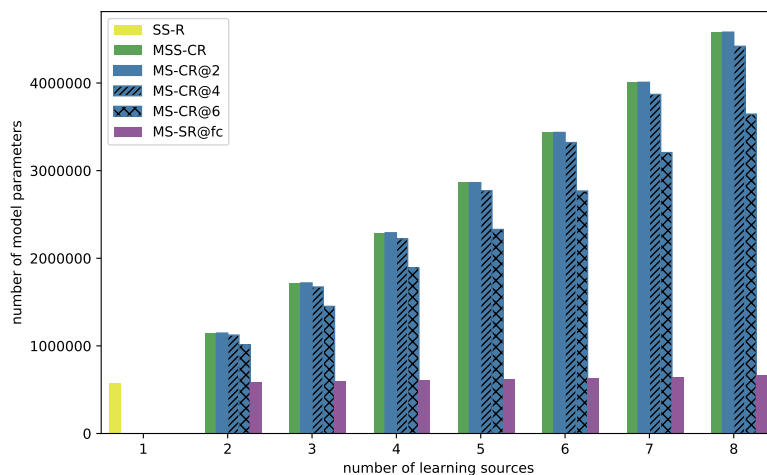


Fig. 11: Number of network parameters by number of learning sources.

see Figure 11 for an overview of necessary model parameters for the different architectures. When using all the learning sources, *MS-CR@6*, which for a considerable part encompasses a shared network architecture and branches out relatively late, has an around 6.3 times larger network size compared to the network size needed for *SS-R*. In contrast, *MS-SR@FC*, which is the most heavily shared MTDTL case, uses a network that is only 1.2 times larger than the network needed for *SS-R*. If network size is a consideration, our results therefore suggest that employing *MS-SR@FC*, one can



achieve a deep representation almost as compact as in the case of *SS-Rs*, which still is based on more learning sources.

Also, while the representations resulting from the *MSS-CR* and various *MS-CR* architectures linearly depend on the chosen number of learning sources  $m$  (see Table 4), for *MS-SR@FC*, which has a fixed dimensionality of  $d$  independent of  $m$ , we do notice increasing performance as more learning sources are used. This implies that under MTDTL setups, the network does learn as much as possible from the multiple sources, even in case of fixed network capacity.

### 5.3 Single-Source vs. Multi-Source

Table 6: Variance components (in standard deviation units) of the learning sources, within each of the evaluation tasks. Largest per task in bold face.

	Ballroom	EmotionAro	EmotionVal	FMA	GTZAN	IRMAS	ThisIsMyJam
self	0.0218	0.0102	<b>0.0212</b>	<b>0.0148</b>	0.0188	0.0087	0.0007
year	0.0106	0.0040	0.0134	0.0059	0.0031	0.0064	<0.0001
bpm	<b>0.1098</b>	<0.0001	0.0173	0.0111	<b>0.0201</b>	<b>0.0227</b>	<0.0001
taste	0.0066	<0.0001	0.0079	<0.0001	<0.0001	<0.0001	0.0007
tag	<0.0001	<b>0.0131</b>	0.0029	0.0060	0.0167	0.0106	0.0005
lyrics	<0.0001	0.0067	<0.0001	<0.0001	<0.0001	<0.0001	<0.0001
cdr_tag	<0.0001	0.0027	<0.0001	<0.0001	0.0122	0.0101	0.0006
artist	0.0037	0.0066	0.0053	0.0042	0.0160	0.0152	<b>0.0013</b>

The evidence so far suggests that, *on average*, learning from multiple sources leads to better performance than learning from a single source. However, it could be possible that the *SS-R* representation with the best learning source for the given task still performs better than a multi-source alternative. In fact, in Fig. 8, in many cases it appears that the best *SS-R* representation (black circles at  $x = 1$ ) already perform quite well compared to the more sophisticated alternatives. Fig. 12 presents similar scatter plots, but now explicitly differentiating between representations using the single best source (empty circles) and representations not using it (filled circles). The results suggest that even if the strongest learning source for the specific task is not used, the others tend to compensate for it to a large extent. As the plot shows, the variability for low numbers of learning sources is larger when not using the strongest source, but as more sources are added, this variability reduces.

For each evaluation dataset, we also computed the variance component due to each of the learning sources [78]. A large variance due to one of the sources means that, on average and for that specific task, there is a large difference in performance between having that source or not. Table 6 shows all variance components, highlighting the per-task largest. Apart from *bpm* in the Ballroom dataset, there is no clear evidence that one single source is specially important for a given evaluation task, which suggests that in general, there is not a single source that one would use by default.

In addition, we observe that the sources with largest variance are not generally the sources that obtain the best results by themselves in an *SS-R* representation (see Fig. 6). We examined this relationship further by calculating the correlation between the per-task variance components (a column in Table 6) and the per-task performance of the corresponding *SS-Rs* (the bar plot scores

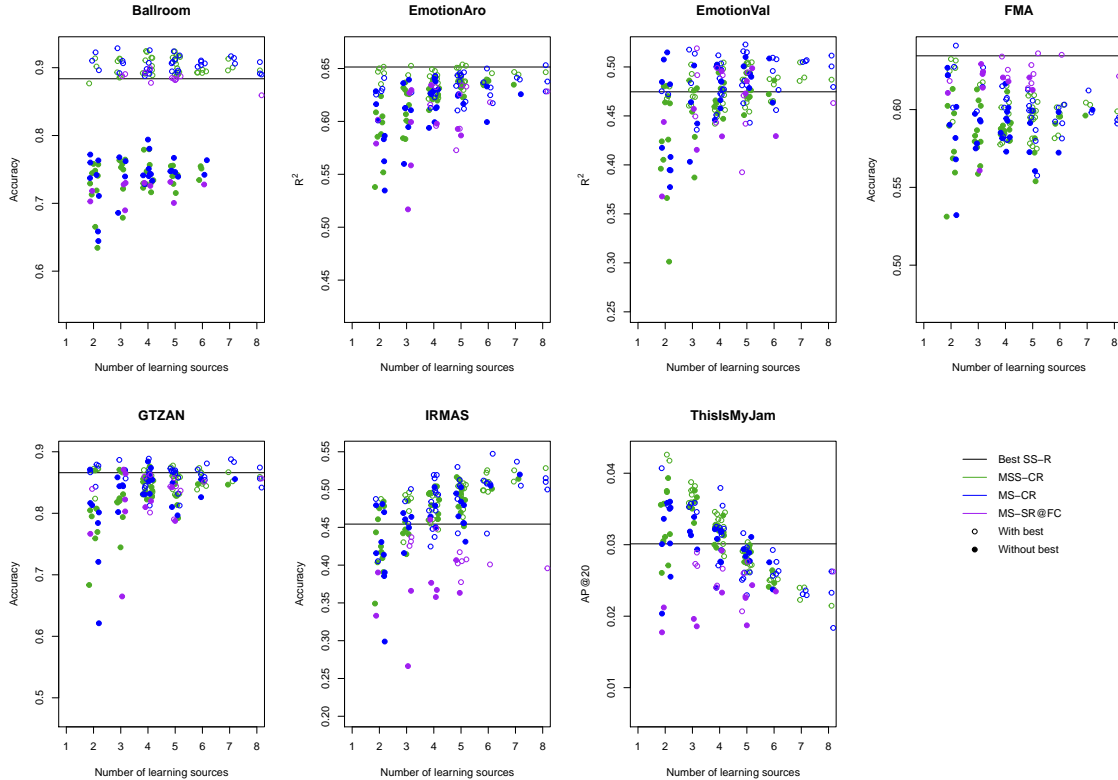


Fig. 12: Multi-source transfer performance with (empty circles) and without (filled circles) best performing single source.

in Fig. 6). The mean Spearman correlation is  $-0.0597$ , evidencing the lack of direct relationship. Fig. 13 further shows this by plotting the rank statistics for each dataset.

This result implies that even if some *SS-R* is particularly strong for a given task, when considering more complex fusion architectures, the presence of that one source is not necessarily important as the other sources make up for its absence. This is especially important in practical terms, because different tasks generally have different best sources, and practitioners rarely have sufficient domain knowledge to select them up front. Also, and unlike the Ballroom dataset, many real-world problems are not easily solved with a single feature. Therefore, choosing a general representation based on multiple sources is a much simpler way to proceed which still yields comparable results.

In other words, if ‘a single deep representation to rule them all’ should be pre-trained, it will be advisable to base this representation on multiple learning sources. At the same time, given that *MSS-CR* representations also generally show strong performance (albeit that they will bring high dimensionality), and that they will come ‘for free’ as soon as *SS-R* networks are trained, alternatively, we could imagine an ecosystem in which the community could pre-train and release many *SS-R* networks for different individual sources in a distributed way, and practitioners can then collect these into *MSS-CR* representations, without the need for retraining.

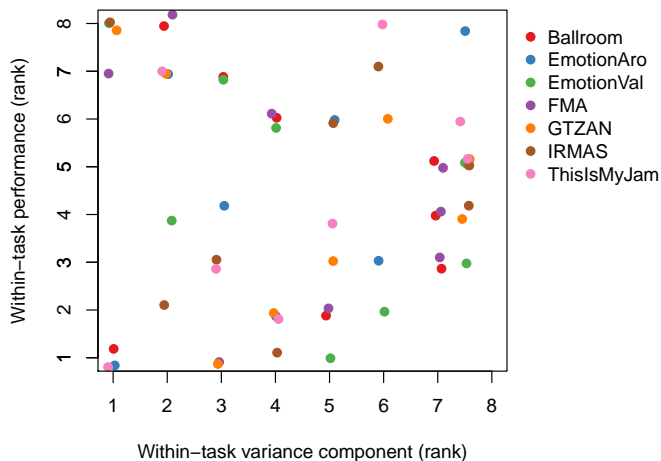


Fig. 13: Rank correlation between within-task performance and variance component.

#### 5.4 Multiple Explanatory Factors

By training representation models on multiple learning sources in the way we did, our hope is that the representation will reflect latent semantic facets that will ultimately allow for semantic explainability. In Fig. 14, we show a visualization that suggests this indeed may be possible. More specifically, we consider one of our *MS-CR* models trained on 7 learning sources. For each task-specific block of the representation, using the task-specific *fc-out* layers, we can predict a factor distribution  $z^t$  for each of the tasks. Then, from the predicted  $z^t$ , one can either map this back on the original learning targets  $y^t$ , or simply consider the strongest predicted topics (which we visualized in Fig. 14), to relate the representation to human-understandable facets or descriptions.

Note that, as soon as a representation network model will be adapted to an unseen new task through transfer learning (as we did for evaluation), the *fc-out* layer can not be used to obtain the  $z^t$ , since the lower layers will then be fine-tuned to another task. However, we hypothesize it may be possible that the semantic explainability can still be preserved, if fine-tuning is jointly conducted with the learning sources used during the pre-training time.

## 6 Conclusion

In this paper, we have investigated the effect of different strategies to learn music representations with deep networks, considering multiple learning sources and different network architectures with varying degrees of shared information. Our main research questions are to answer how the number and combination of learning sources (**RQ1**), and different configurations of the shared architecture (**RQ2**) affect effectiveness (**RQ3**) of the learned deep music representation. As a consequence, we conducted an experiment training 90 neural network models with different combinations of learning

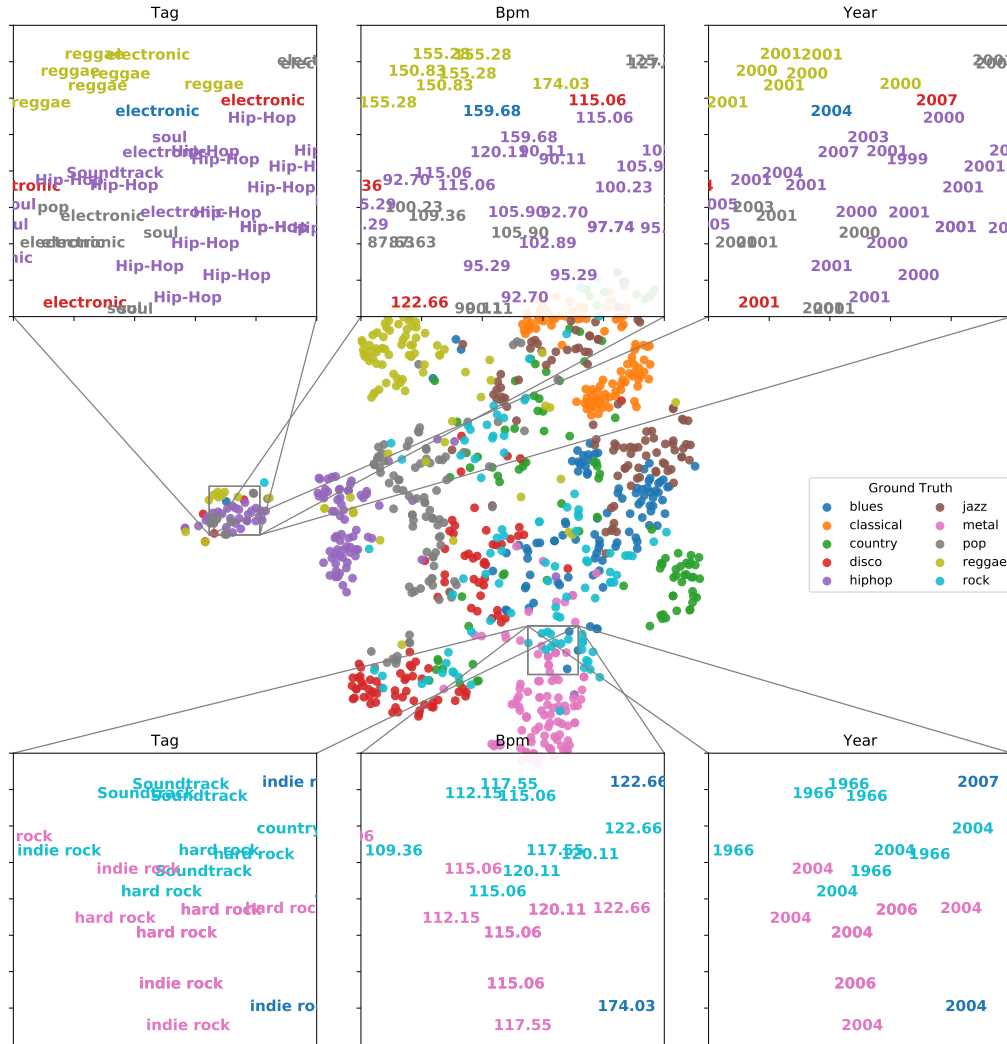


Fig. 14: Potential semantic explainability of DTMTL music representations. Here, we provide an t-SNE visualization [79], plotting 2-dimensional coordinates of each sample from the GTZAN evaluation task, as resulting from an *MS-CR* representation from one of the models trained with 7 learning sources. In the zoomed-in panes, we overlay the strongest topic model terms in  $z^t$ , for various types of tasks from various types of learning sources.

sources and architectures, which led an evaluation of 169 different representation variants, also taking into account concatenations of individually trained networks.

After an extensive empirical analysis, we can summarize our findings as follows:

- **RQ1** The number of learning sources positively affect the effectiveness of a learned deep music representation, although representations based on a single knowledge source will already be effective in specialized cases (e.g. the Ballroom dataset).
- **RQ2** In terms of architecture, larger models with less shared information (*MS-CR@2*, *MSS-CR*) show a tentative trend of stronger performance, although this was not statistically significant yet.
- **RQ3** Running our experiments on multiple learning and evaluation tasks, observed effects due to the choice of evaluation dataset are more significant than of the choice of architecture.

Our findings give various pointers to useful future work. First of all, ‘generality’ is difficult to define in the music domain, maybe more so than in CV or NLP, in which lower-level information atoms may be less multifaceted in nature (e.g. lower-level representations of visual objects naturally extend to many vision tasks, while an equivalent in music is harder to pinpoint). In case of clear task-specific data skews, practitioners should be pragmatic about this.

While the tentative trends we observed for different architectures were not significant in our current experiments, at the same time, due to resource capacity, we used an optimal but limited set of experimental runs, and sub-sampled dataset slices for training and evaluation. We would expect that the observed trends will settle more strongly as more experimental runs on larger datasets will be considered, potentially also considering further choices of topology and branching strategies in the neural network architectures.

Finally, in our current work, we still largely considered MTDTL as a ‘black box’ operation, trying to learn *how* MTDTL can be effective. However, the original reason for starting this work was not only to yield an effective general-purpose representation, but one that also would be semantically interpretable according to different semantic facets. We showed some early evidence our representation networks may be capable of picking up such facets; however, considerable future work will be needed into more in-depth analysis techniques of *what* the deep representations actually learned.

**Acknowledgements** This work was carried out on the Dutch national e-infrastructure with the support of SURF Cooperative. We further thank the CDR for having provided their album-level genre annotations for our experiments. Finally, We thank Keunwoo Choi for the discussion and all the help regarding the implementation of his work.

*Conflict of interest: Jaehun Kim, Julián Urbano, Cynthia C. S. Liem and Alan Hanjalic state that there are no conflicts of interest.*

## References

1. Michael A. Casey, Remco Veltkamp, Masataka Goto, Marc Leman, Christophe Rhodes, and Malcolm Slaney. Content-based music information retrieval: Current directions and future challenges. *Proceedings of the IEEE*, 96(4):668–696, 2008. ISSN 00189219. doi: 10.1109/JPROC.2008.916370.
2. Philippe Hamel and Douglas Eck. Learning Features from Music Audio with Deep Belief Networks. *International Society for Music Information Retrieval Conference (ISMIR)*, (Ismir): 339–344, 2010.

3. Nicolas Boulanger-Lewandowski, Pascal Vincent, and Yoshua Bengio. Modeling Temporal Dependencies in High-Dimensional Sequences: Application to Polyphonic Music Generation and Transcription. *Proceedings of the 29th International Conference on Machine Learning (ICML-12)*, (Cd):1159–1166, 2012.
4. Jan Schlüter and Sebastian Böck. Improved Musical Onset Detection with Convolutional Neural Networks. In *Proceedings of the IEEE International Conference on Acoustics, Speech, and Signal Processing (ICASSP 2014)*, Florence, Italy, 5 2014.
5. Keunwoo Choi, George Fazekas, and Mark Sandler. Automatic tagging using deep convolutional neural networks. *International Society for Music Information Retrieval Conference*, pages 805–811, 2016.
6. Aaron van den Oord, Sander Dieleman, and Benjamin Schrauwen. Deep content-based music recommendation. *Electronics and Information Systems department (ELIS)*, page 9, 2013. ISSN 10495258. doi: 10.1109/MMUL.2011.34.van. URL <http://papers.nips.cc/paper/5004-deep-content-based-music-recommendation.pdf>.
7. Pritish Chandna, Marius Miron, Jordi Janer, and Emilia Gómez. Monoaural audio source separation using deep convolutional neural networks. In *International Conference on Latent Variable Analysis and Signal Separation*, pages 258–266. Springer, 2017.
8. Karen Simonyan and Andrew Zisserman. Very Deep Convolutional Networks for Large-Scale Image Recognition. *arXiv preprint*, pages 1–10, 2014. ISSN 09505849. doi: 10.1016/j.infsof.2008.09.005. URL <http://arxiv.org/abs/1409.1556>.
9. Kaiming He, Xiangyu Zhang, Shaoqing Ren, and Jian Sun. Deep Residual Learning for Image Recognition.
10. Christian Szegedy, Wei Liu, Yangqing Jia, Pierre Sermanet, Scott Reed, Dragomir Anguelov, Dumitru Erhan, Vincent Vanhoucke, and Andrew Rabinovich. Going deeper with convolutions. *Proceedings of the IEEE Computer Society Conference on Computer Vision and Pattern Recognition*, 07-12-June:1–9, 2015. ISSN 10636919. doi: 10.1109/CVPR.2015.7298594.
11. Tomas Mikolov, Kai Chen, Greg Corrado, and Jeffrey Dean. Efficient Estimation of Word Representations in Vector Space. pages 1–12, 2013. ISSN 15324435. doi: 10.1162/153244303322533223. URL <http://arxiv.org/abs/1301.3781>.
12. Sander Dieleman, Philmon Brakel, and Benjamin Schrauwen. Audio-based Music Classification with a Pretrained Convolutional Network. *International Society for Music Information Retrieval Conference (ISMIR)*, (Ismir):669–674, 2011. URL <https://biblio.ugent.be/publication/1989534>.
13. Keunwoo Choi, George Fazekas, Mark Sandler, and Kyunghyun Cho. Transfer learning for music classification and regression tasks. In *The 18th International Society of Music Information Retrieval (ISMIR) Conference 2017, Suzhou, China*. International Society of Music Information Retrieval, 2017.
14. Aron Van Den Oord, Sander Dieleman, and Benjamin Schrauwen. Transfer learning by supervised pre-training for audio-based music classification. In *Conference of the International Society for Music Information Retrieval (ISMIR 2014)*, 2014.
15. Yu Zhang and Qiang Yang. A Survey on Multi-Task Learning. pages 1–20, 2017. URL <http://arxiv.org/abs/1707.08114>.
16. Yoshua Bengio, Aaron Courville, and Pascal Vincent. Representation Learning: A Review and New Perspectives. *arXiv:1206.5538 [cs]*, 35(8):1798–1828, 2012. ISSN 15324435. doi: 10.1145/1756006.1756025. URL <http://arxiv.org/abs/1206.5538> <http://www.arxiv.org/pdf/1206.5538.pdf>.

17. Wu Liu, Tao Mei, Yongdong Zhang, Cherry Che, and Jiebo Luo. Multi-task deep visual-semantic embedding for video thumbnail selection. In *Proceedings of the IEEE Computer Society Conference on Computer Vision and Pattern Recognition*, 2015. ISBN 9781467369640. doi: 10.1109/CVPR.2015.7298994.
18. Joachim Bingel and Anders Søgaard. Identifying beneficial task relations for multi-task learning in deep neural networks. *Proceedings of the 15th Conference of the European Chapter of the Association for Computational Linguistics*, 2(2016):164–169, 2017. URL [http://eacl2017.org/images/site/Proceeding/book\\_short.pdf](http://eacl2017.org/images/site/Proceeding/book_short.pdf).
19. Sijin Li, Zhi-Qiang Liu, and Antoni B Chan. Heterogeneous multi-task learning for human pose estimation with deep convolutional neural network. In *Proceedings of the IEEE Conference on Computer Vision and Pattern Recognition Workshops*, pages 482–489, 2014.
20. Wenlu Zhang, Rongjian Li, Tao Zeng, Qian Sun, Sudhir Kumar, Jieping Ye, and Shuiwang Ji. Deep Model Based Transfer and Multi-Task Learning for Biological Image Analysis. In *Proceedings of the 21th ACM SIGKDD International Conference on Knowledge Discovery and Data Mining - KDD '15*, 2015. ISBN 9781450336642. doi: 10.1145/2783258.2783304.
21. Zhanpeng Zhang, Ping Luo, Chen Change Loy, and Xiaoou Tang. Facial Landmark Detection by Deep Multi-task Learning.
22. Il-young Jeong and Kyogu Lee. Learning Temporal Features Using a Deep Neural Network and its Application to Music Genres Classification. *Ismir*, pages 434–440, 2016.
23. Aaron van den Oord, Sander Dieleman, Heiga Zen, Karen Simonyan, Oriol Vinyals, Alex Graves, Nal Kalchbrenner, Andrew Senior, and Koray Kavukcuoglu. WaveNet: A Generative Model for Raw Audio. pages 1–15, 2016. URL <http://arxiv.org/abs/1609.03499>.
24. Jesse Engel, Cinjon Resnick, Adam Roberts, Sander Dieleman, Douglas Eck, Karen Simonyan, and Mohammad Norouzi. Neural Audio Synthesis of Musical Notes with WaveNet Autoencoders. 2017. URL <http://arxiv.org/abs/1704.01279>.
25. Rich Caruana. Multitask Learning \*. *Machine Learning*, 28:41–75, 1997. ISSN 1573-0565. doi: 10.1023/A:1007379606734.
26. Ishan Misra, Abhinav Shrivastava, Abhinav Gupta, and Martial Hebert. Cross-stitch networks for multi-task learning. In *Proceedings of the IEEE Conference on Computer Vision and Pattern Recognition*, pages 3994–4003, 2016.
27. Yusuf Aytar, Carl Vondrick, and Antonio Torralba. Soundnet: Learning sound representations from unlabeled video. In *Advances in Neural Information Processing Systems*, 2016.
28. Thierry Bertin-Mahieux, Daniel P W Ellis, Brian Whitman, and Paul Lamere. The Million Song Dataset. In *Proceedings of the 12th International Conference on Music Information Retrieval ({ISMIR} 2011)*, 2011.
29. Yoshua Bengio, Pascal Lamblin, Dan Popovici, and Hugo Larochelle. Greedy layer-wise training of deep networks. In *Advances in neural information processing systems*, pages 153–160, 2007.
30. Pascal Vincent, Hugo Larochelle, Yoshua Bengio, and Pierre-Antoine Manzagol. Extracting and composing robust features with denoising autoencoders. In *Proceedings of the 25th international conference on Machine learning - ICML '08*, 2008. ISBN 9781605582054. doi: 10.1145/1390156.1390294.
31. Paul Smolensky. Information processing in dynamical systems: Foundations of harmony theory. Technical report, COLORADO UNIV AT BOULDER DEPT OF COMPUTER SCIENCE, 1986.
32. Geoffrey E. Hinton, Simon Osindero, and Yee-Whye Teh. A Fast Learning Algorithm for Deep Belief Nets. *Neural Computation*, 18(7):1527–1554, 2006. ISSN 0899-7667. doi:

- 10.1162/neco.2006.18.7.1527. URL <http://www.mitpressjournals.org/doi/10.1162/neco.2006.18.7.1527>.
33. Ian Goodfellow, Jean Pouget-Abadie, Mehdi Mirza, Bing Xu, David Warde-Farley, Sherjil Ozair, Aaron Courville, and Yoshua Bengio. Generative adversarial nets. In *Advances in neural information processing systems*, pages 2672–2680, 2014.
  34. Xufeng Han, Thomas Leung, Yangqing Jia, Rahul Sukthankar, and Alexander C. Berg. Match-Net: Unifying feature and metric learning for patch-based matching. *Proceedings of the IEEE Computer Society Conference on Computer Vision and Pattern Recognition*, 07-12-June:3279–3286, 2015. ISSN 10636919. doi: 10.1109/CVPR.2015.7298948.
  35. Relja Arandjelović and Andrew Zisserman. Look, Listen and Learn. *arXiv:1705.08168v1 [cs]*, 2017. ISSN 00296511. URL <http://arxiv.org/abs/1705.08168v1>.
  36. Yu-Siang Huang, Szu-Yu Chou, and Yi-Hsuan Yang. Similarity Embedding Network for Unsupervised Sequential Pattern Learning by Playing Music Puzzle Games. 2017. URL <http://arxiv.org/abs/1709.04384>.
  37. Gerard Salton. *Introduction to modern information retrieval*. McGraw-Hill, New York, 1983. ISBN 9780070544840.
  38. Paul Lamere. Social Tagging and Music Information Retrieval. *Journal of New Music Research*, 37(2):101–114, 2008. ISSN 0929-8215. doi: 10.1080/09298210802479284.
  39. Jason Weston, Samy Bengio, and Philippe Hamel. Multi-Tasking with Joint Semantic Spaces for Large- Scale Music Annotation and Retrieval Multi-Tasking with Joint Semantic Spaces for Large-Scale Music Annotation and Retrieval. *Journal of New Music Research*, (November 2012):37–41, 2011. ISSN 0929-8215. doi: 10.1080/09298215.2011.603834.
  40. Philippe Hamel, Matthew E P Davies, Kazuyoshi Yoshii, and Masataka Goto. TRANSFER LEARNING IN MIR : SHARING LEARNED LATENT REPRESENTATIONS FOR MUSIC AUDIO CLASSIFICATION AND SIMILARITY. (*Ismir*):9–14, 2013.
  41. Edith Law, Burr Settles, and Tom Mitchell. Learning to Tag using Noisy Labels. *European Conference on Machine Learning*, 2010.
  42. Thomas Hofmann. Probabilistic latent semantic indexing. *Proceedings of the 22nd annual international ACM SIGIR conference on Research and development in information retrieval*, pages 50–57, 1999. ISSN 00032700. doi: 10.1021/ac801303x.
  43. Yoonchang Han, Jaehun Kim, and Kyogu Lee. Deep convolutional neural networks for predominant instrument recognition in polyphonic music. 2016.
  44. Jan Schlüter. Learning To Pinpoint Singing Voice From Weakly Labeled Examples. *Proc. 17th International Society for Music Information Retrieval Conference*, pages 44–50, 2016.
  45. Alex Krizhevsky, Ilya Sutskever, and Hinton Geoffrey E. ImageNet Classification with Deep Convolutional Neural Networks. *Advances in Neural Information Processing Systems 25 (NIPS2012)*, page 19, 2012. ISSN 10495258. doi: 10.1109/5.726791. URL <https://papers.nips.cc/paper/4824-imagenet-classification-with-deep-convolutional-neural-networks.pdf>.
  46. Sander Dieleman and Benjamin Schrauwen. END-TO-END LEARNING FOR MUSIC AUDIO. In *Icassp*, pages 7014–7018, 2014. ISBN 9781479928934.
  47. Navdeep Jaitly and Geoffrey E Hinton. LEARNING A BETTER REPRESENTATION OF SPEECH SOUND WAVES USING RESTRICTED BOLTZMANN MACHINES Navdeep Jaitly , Geoffrey Hinton. *Learning*, 1:1–4, 2011. ISSN 1520-6149. doi: 10.1109/ICASSP.2011.5947700. URL [http://learning.cs.toronto.edu/~hinton/absps/jaitly\\_ICASSP2011.pdf](http://learning.cs.toronto.edu/~hinton/absps/jaitly_ICASSP2011.pdf).



48. Jongpil Lee, Jiyoung Park, Keunhyoung Luke, and Kim Juhan Nam. Sample-Level Deep Convolutional Neural Networks for Music Auto-Tagging using Raw Waveforms. *arXiv*, 2017. URL <https://arxiv.org/pdf/1703.01789.pdf>.
49. Vinod Nair and Geoffrey E Hinton. Rectified Linear Units Improve Restricted Boltzmann Machines. *Proceedings of the 27th International Conference on Machine Learning*, (3):807–814, 2010. ISSN 1935-8237. doi: 10.1.1.165.6419.
50. Sergey Ioffe and Christian Szegedy. Batch Normalization: Accelerating Deep Network Training by Reducing Internal Covariate Shift. 2015.
51. Nitish Srivastava, Geoffrey Hinton, Alex Krizhevsky, Ilya Sutskever, and Ruslan Salakhutdinov. Dropout: A Simple Way to Prevent Neural Networks from Overfitting. *Journal of Machine Learning Research*, 15:1929–1958, 2014. ISSN 15337928. doi: 10.1214/12-AOS1000.
52. Juhan Nam, Jorge Herrera, Malcolm Slaney, and Julius Smith. Learning Sparse Feature Representations for Music Annotation and Retrieval. *International Conference on Music Information Retrieval*, (Ismir):565–570, 2012.
53. Keunwoo Choi, George Fazekas, Kyunghyun Cho, and Mark Sandler. A Comparison on Audio Signal Preprocessing Methods for Deep Neural Networks on Music Tagging. 2017. URL <http://arxiv.org/abs/1709.01922>.
54. Monika Doerfler, Thomas Grill, Roswitha Bammer, and Arthur Flexer. Basic Filters for Convolutional Neural Networks: Training or Design? pages 1–23, 2017. URL <http://arxiv.org/abs/1709.02291>.
55. Kaiming He, Xiangyu Zhang, Shaoqing Ren, and Jian Sun. Deep residual learning for image recognition. In *Proceedings of the IEEE conference on computer vision and pattern recognition*, pages 770–778, 2016.
56. Diederik P. Kingma and Jimmy Ba. Adam: A Method for Stochastic Optimization. pages 1–15, 2014. ISSN 09252312. doi: <http://doi.acm.org.ezproxy.lib.ucf.edu/10.1145/1830483.1830503>. URL <http://arxiv.org/abs/1412.6980>.
57. Sander Dieleman, Jan Schlüter, Colin Raffel, Eben Olson, Sren Kaae Sønderby, Daniel Nouri, and others. Lasagne: First release., 8 2015. URL <http://dx.doi.org/10.5281/zenodo.27878>.
58. Theano Development Team. Theano: A {Python} framework for fast computation of mathematical expressions. *arXiv e-prints*, abs/1605.0, 5 2016. URL <http://arxiv.org/abs/1605.02688>.
59. Bart van Merriënboer, Dzmitry Bahdanau, Vincent Dumoulin, Dmitriy Serdyuk, David Warde-Farley, Jan Chorowski, and Yoshua Bengio. Blocks and Fuel: Frameworks for deep learning. pages 1–5, 2015. URL <http://arxiv.org/abs/1506.00619>.
60. Fabian Pedregosa, Gal Varoquaux, Alexandre Gramfort, Vincent Michel, Bertrand Thirion, Olivier Grisel, Mathieu Blondel, Peter Prettenhofer, Ron Weiss, Vincent Dubourg, Jake Vanderplas, Alexandre Passos, David Cournapeau, Matthieu Brucher, Matthieu Perrot, and douard Duchesnay. Scikit-learn: Machine Learning in Python. *Journal of Machine Learning Research*, 12:2825–2830, 2012. ISSN 15324435. doi: 10.1007/s13398-014-0173-7.2. URL <http://dl.acm.org/citation.cfm?id=2078195%5Cnhttp://arxiv.org/abs/1201.0490>.
61. Brian Mcfee, Colin Raffel, Dawen Liang, Daniel P W Ellis, Matt Mcvicar, Eric Battenberg, and Oriol Nieto. librosa: Audio and Music Signal Analysis in Python. *PROC. OF THE 14th PYTHON IN SCIENCE CONF*, 2015.
62. Douglas C Montgomery. *Design and Analysis of Experiments*. Wiley, 8th edition, 2012.
63. George Tzanetakis and Perry Cook. Musical genre classification of audio signals: IEEE. *IEEE transactions on Speech and Audio Processing*, 10(5):292–302, 2002. ISSN 10636676. doi: 10.1109/TSA.2002.800560.

64. Michaël Defferrard, Kirell Benzi, Pierre Vandergheynst, and Xavier Bresson. Fma: A dataset for music analysis. In *18th International Society for Music Information Retrieval Conference*, 2017.
65. Bob L. Sturm. The state of the art ten years after a state of the art: Future research in music information retrieval. *Journal of New Music Research*, 43(2):147–172, 2014. doi: 10.1080/09298215.2014.894533. URL <https://doi.org/10.1080/09298215.2014.894533>.
66. Fabien Gouyon, Anssi Klapuri, Simon Dixon, Miguel Alonso, George Tzanetakis, Christian Uhle, and Pedro Cano. An experimental comparison of audio tempo induction algorithms. *IEEE Transactions on Audio, Speech and Language Processing*, 14(5):1832–1844, 2006. ISSN 15587916. doi: 10.1109/TSA.2005.858509.
67. Bob L. Sturm. The "horse" inside: Seeking causes behind the behaviors of music content analysis systems. *Computers in Entertainment*, 14:3:1–3:32, 2016.
68. Jj Bosch, Jordi Janer, Ferdinand Fuhrmann, and Perfecto Herrera. A Comparison of Sound Segregation Techniques for Predominant Instrument Recognition in Musical Audio Signals. *13th International Society for Music Information Retrieval Conference*, (Ismir):559–564, 2012. URL <http://mtg.upf.es/system/files/publications/Bosch-ISMIR2012.pdf>.
69. Mohammad Soleymani, Micheal N. Caro, Erik M. Schmidt, Cheng-Ya Sha, and Yi-Hsuan Yang. 1000 Songs for Emotional Analysis of Music. *Proceedings of the 2nd ACM international workshop on Crowdsourcing for multimedia - CrowdMM '13*, pages 1–6, 2013. doi: 10.1145/2506364.2506365. URL <http://dl.acm.org/citation.cfm?doid=2506364.2506365>.
70. J Posner, J A Russell, and B S Peterson. The circumplex model of affect: An integrative approach to affective neuroscience, cognitive development, and psychopathology. *Dev Psychopathol*, 17(03):715–734, 2005. ISSN 1469-2198. doi: doi:10.1017/S0954579405050340. URL <http://journals.cambridge.org/action/displayAbstract?fromPage=online&aid=349120&fulltextType=RA&fileId=S0954579405050340>.
71. Andreas Jansson. This Is My Jam Data Dump. 2015.
72. Dawen Liang. Content-Aware Collaborative Music Recommendation Using Pre-trained Neural Networks. *ISMIR 2015: Proceedings of the 16th International Society for Music Information Retrieval Conference*, pages 295–301, 2014.
73. Corinna Cortes and Vladimir Vapnik. Support-Vector Networks. *Machine Learning*, 20(3): 273–297, 1995. ISSN 15730565. doi: 10.1023/A:1022627411411.
74. Alex J Smola and Bernhard Sc Olkopf. A tutorial on support vector regression \*. *Statistics and Computing*, 14:199–222, 2004. ISSN 0960-3174. doi: 10.1023/B:STCO.0000035301.49549.88.
75. Chih-Chung Chang and Chih-Jen Lin. {LIBSVM}: A library for support vector machines. *ACM Transactions on Intelligent Systems and Technology*, 2(3):27:1–27:27, 2011.
76. Yue Shi, Martha Larson, and Alan Hanjalic. Mining mood-specific movie similarity with matrix factorization for context-aware recommendation. In *Proceedings of the workshop on context-aware movie recommendation*, pages 34–40. ACM, 2010.
77. Andrew Gelman and Jennifer Hill. *Data Analysis Using Regression and Multilevel/Hierarchical Models*. 2006.
78. SR Searle, G Casella, and CE McCulloch. Variance components. *Wiley Series in Probability and Statistics. Total de registros: 1 BD INIA Ayuda MegaBase Agropecuaria Alianza SIDALC*, 2006.
79. L J P Van Der Maaten and G E Hinton. Visualizing high-dimensional data using t-sne. *Journal of Machine Learning Research*, 9:2579–2605, 2008. ISSN 1532-4435. doi: 10.1007/s10479-011-0841-3. URL <https://lvdmaaten.github.io/publications/papers/>

---

JMLR\_2008.pdf%0Ahttp://www.ncbi.nlm.nih.gov/entrez/query.fcgi?db=pubmed&cmd=Retrieve&dopt=AbstractPlus&list\_uids=7911431479148734548related:V0iAgwMNY20J.